l'Observatoire de Paris | LUTH
Laboratoire Univers et Théories

How we can test fundamental physics with Cosmology?

Eloisa Menegoni

Meudon, 18 December 2013

OUTLINE

- **Cosmic Microwave Background radiation**

- **Epoch of Recombination**

- **Data analysis/Results/Planck**

- **Next projects...**

The Cosmic Microwave Background

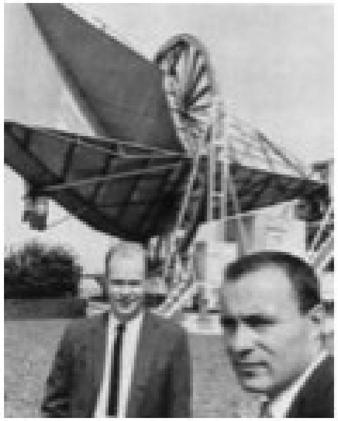

Discovered By Penzias and Wilson in 1965.

It is an image of the universe at the time of recombination (near baryon-photons decoupling), when the universe was just a few thousand years old (z~1000).

The CMB frequency spectrum is a perfect blackbody at T=2.73 K: this is an outstanding confirmation of the hot big bang model.

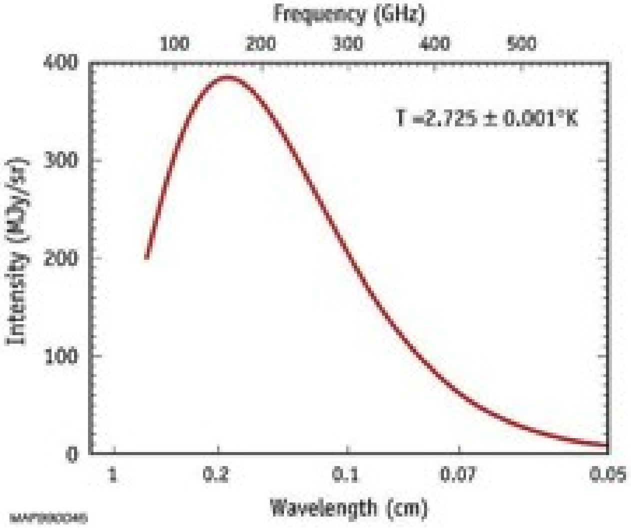

Why we use CMB anisotropies ?

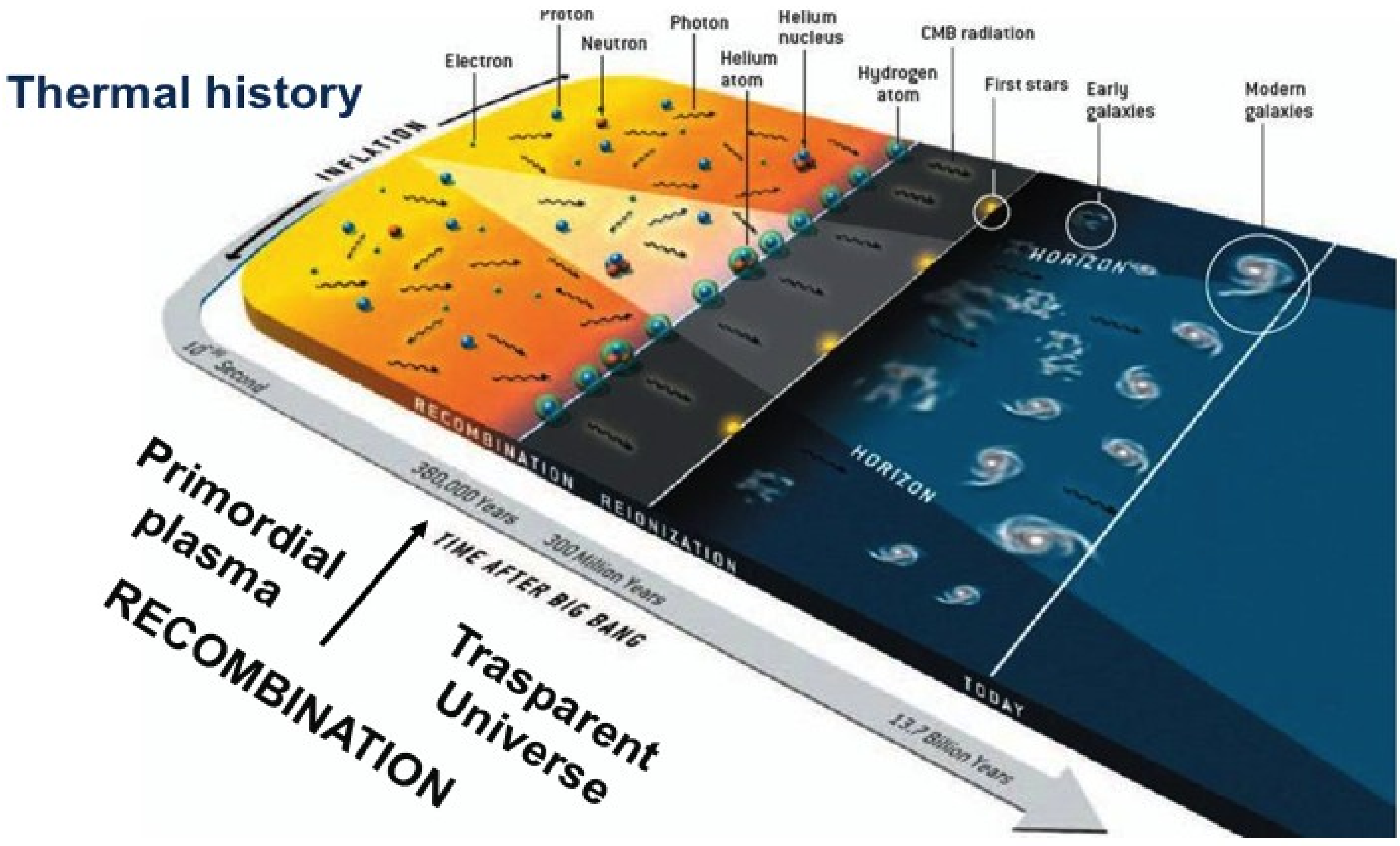

The Microwave Sky

COBE

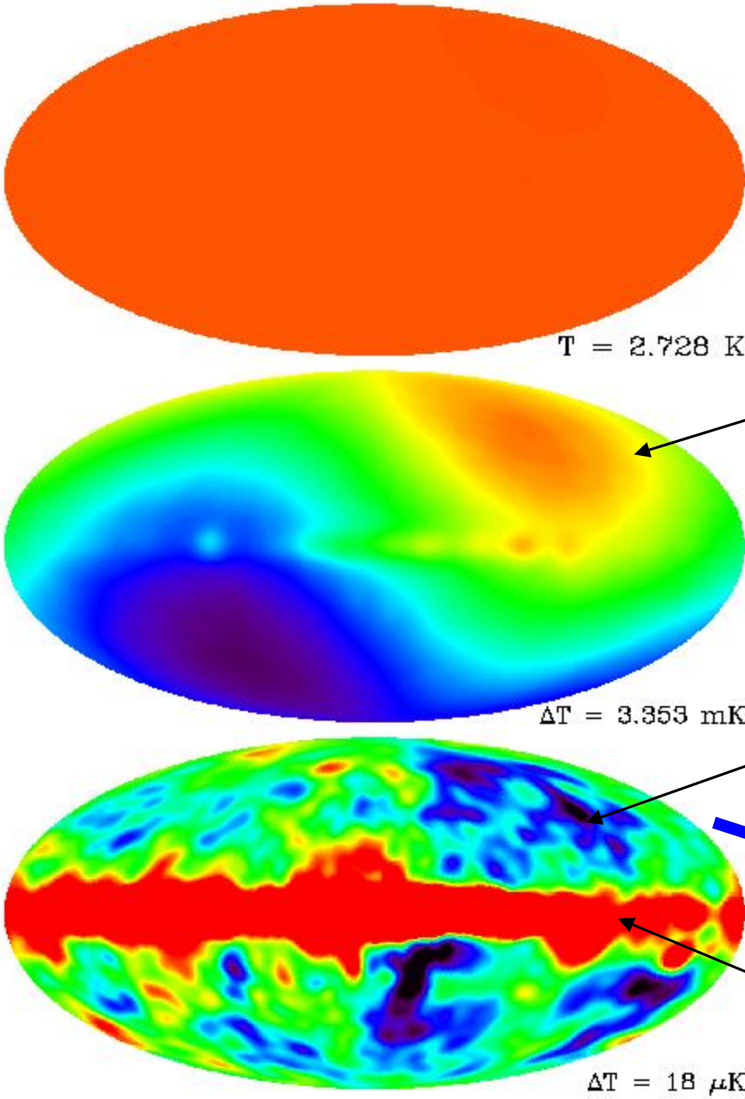

Uniform...

Dipole...

Imprint left by primordial tiny density inhomogeneities (z~1000)..

Galaxy (z=0)

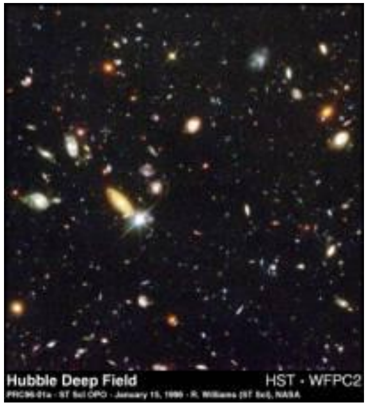

Planck 2013 results. I. Overview of products and scientific results [arXiv:1303.5062].

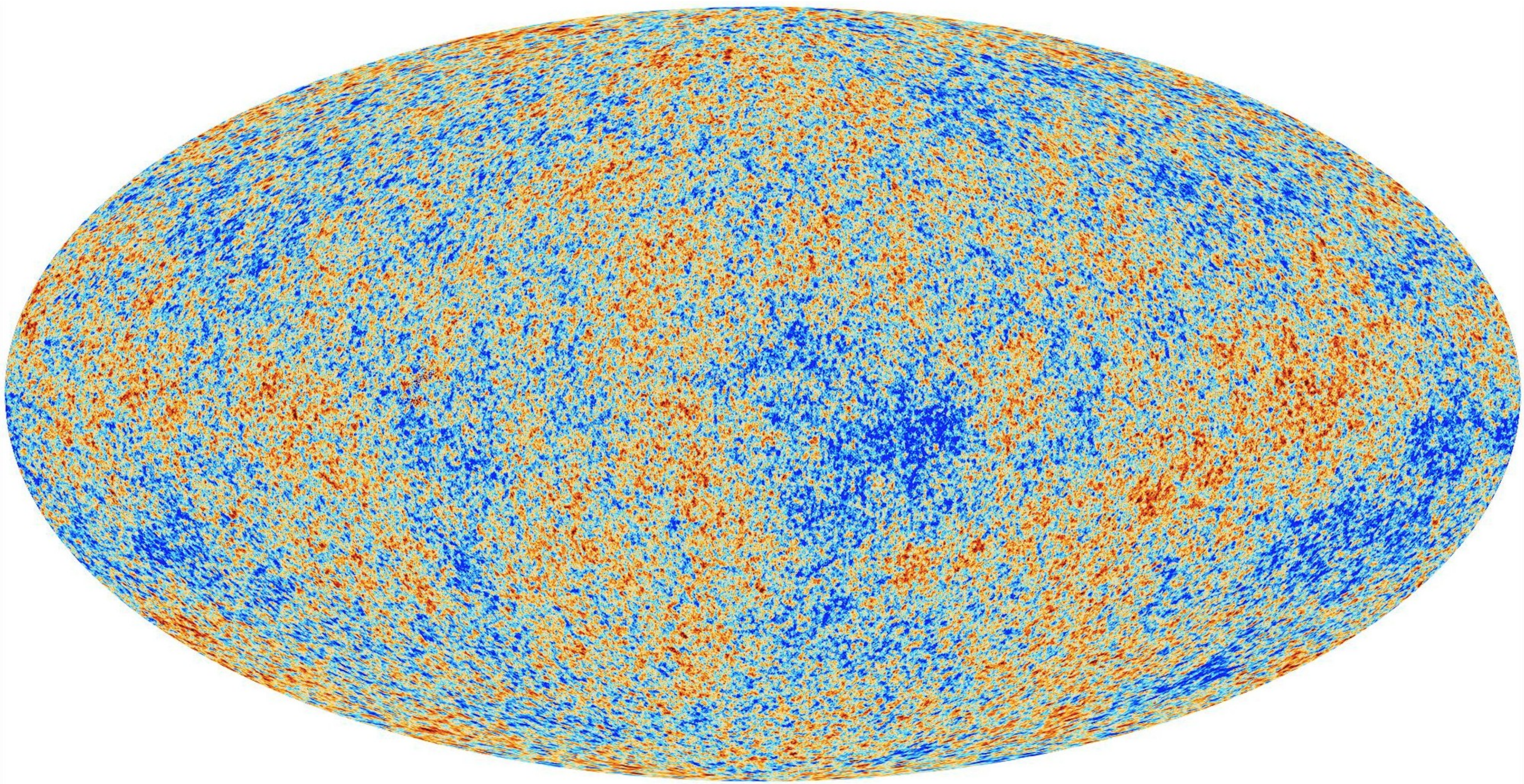

The CMB Angular Power Spectrum

The main reason of this success relies on the existance of a highly predictable theoretical model that describes the CMB anisotropies.
The most important theoretical prediction is the CMB anisotropy angular power spectrum.
i.e. you consider a two point correlation function
For the anisotropies in the sky, you expand
the correlation function in Legendre polinomials
(i.e. there is non azimuthal dependence for
The anisotropies) and the model predict
a value of the Legendre coefficient in function
of the order l as in figure.

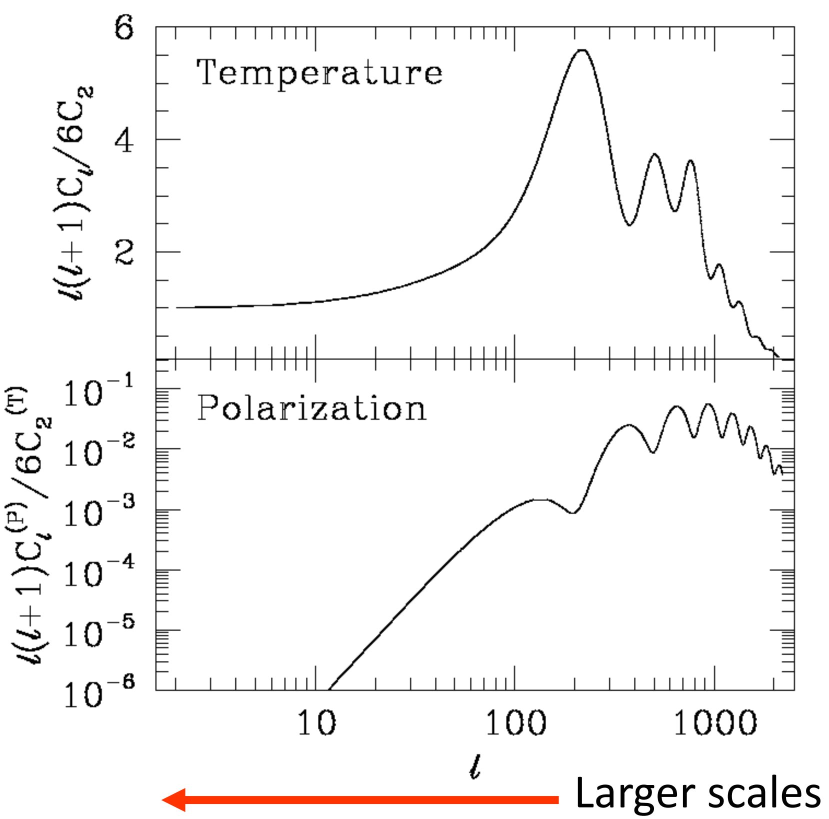

Small l's correspond to large angular scales,
while large l's correspond to small angular scales.

We can correlate not only temperature but
also polarization.

$$\left\langle \frac{\Delta T}{T}(\vec{\gamma}_1)\frac{\Delta T}{T}(\vec{\gamma}_2)\right\rangle = \frac{1}{2\pi}\sum_{\ell}(2\ell+1)C_\ell P_\ell(\vec{\gamma}_1\cdot\vec{\gamma}_2)$$

WMAP

Theory and Experimental data are in spectacular agreement !

We can use the CMB data to constrain the parameter of the model !

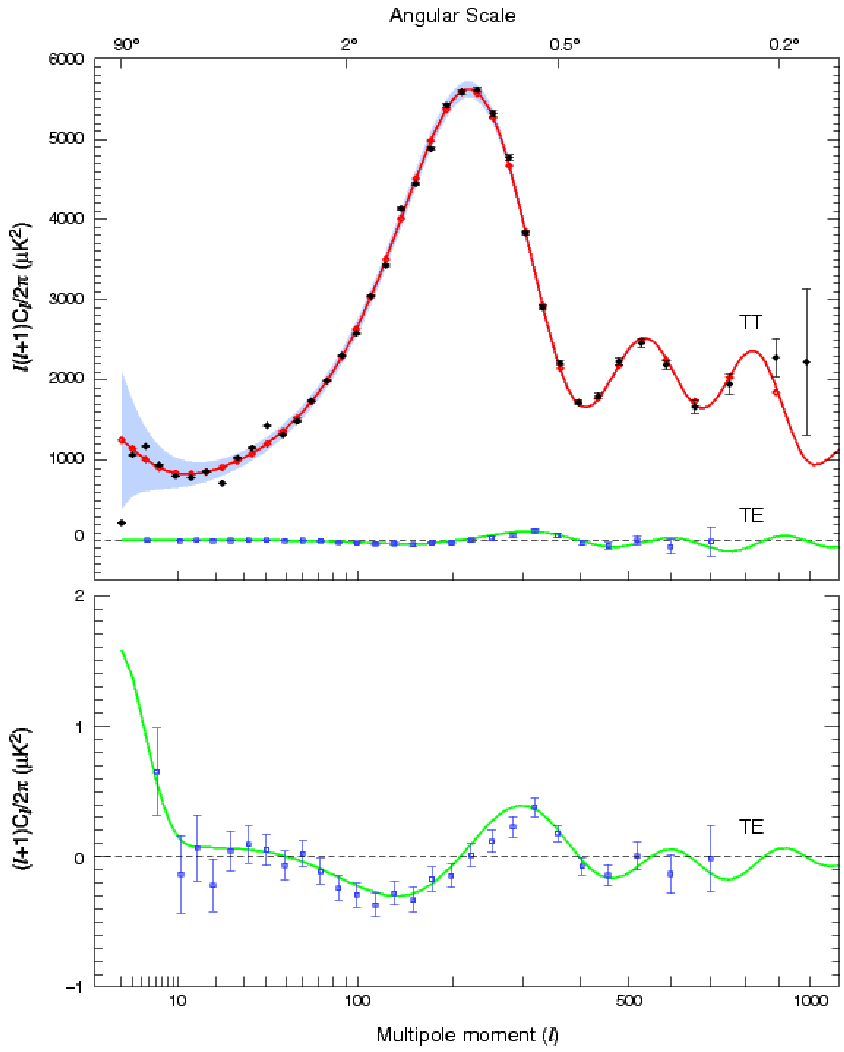

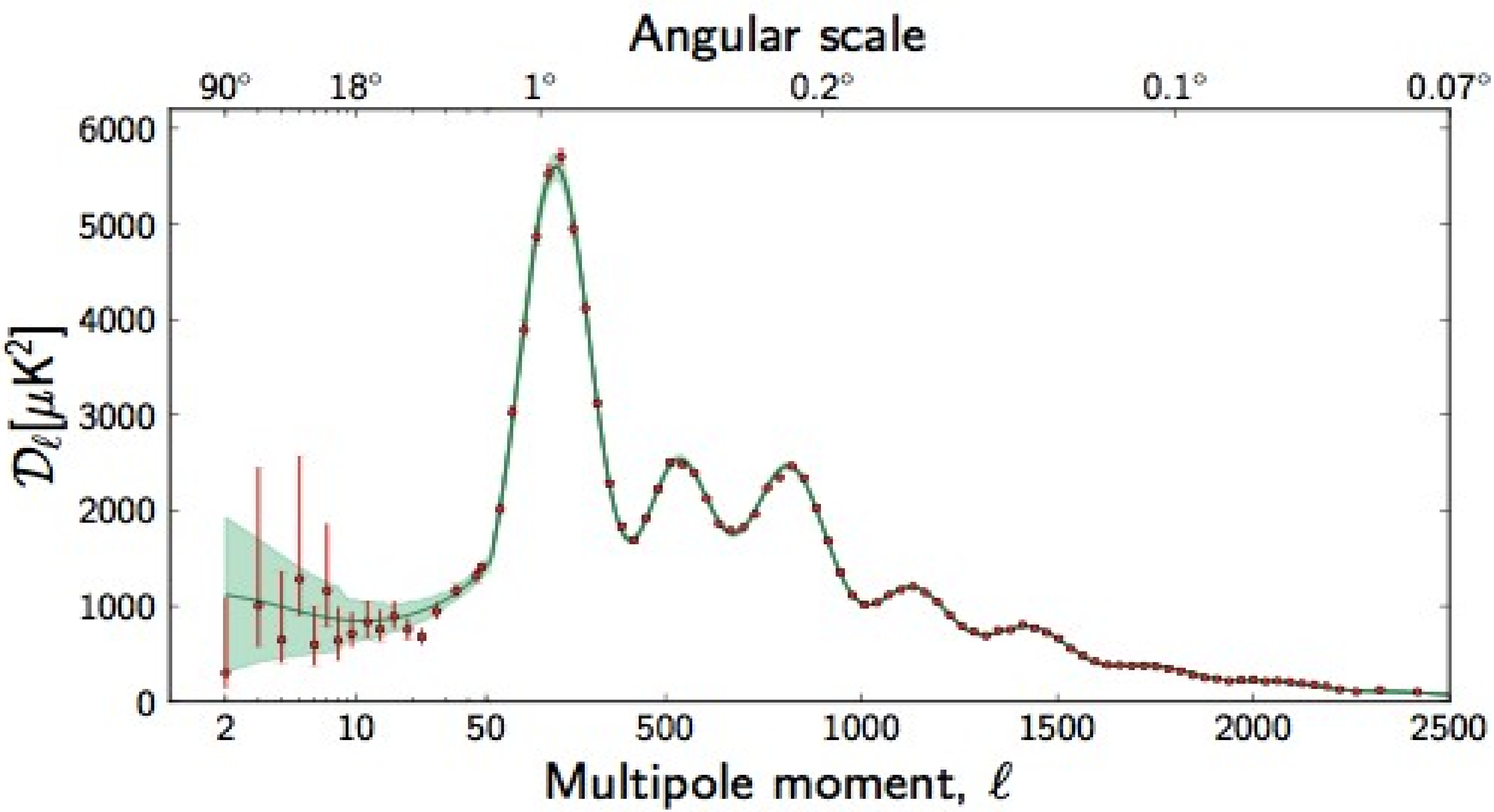

Planck collaboration [2013 Submitted to A&A]
arXiv:1303.5075

A Planck view

FIG 1.2.—*Planck* focal plane unit. The HFI is inserted into the ring formed by the LFI horns, and includes thermal stages at 18 K, 4 K, 2 K and 0.1 K. The cold LFI unit (20 K) is attached by bipods to the telescope structure.

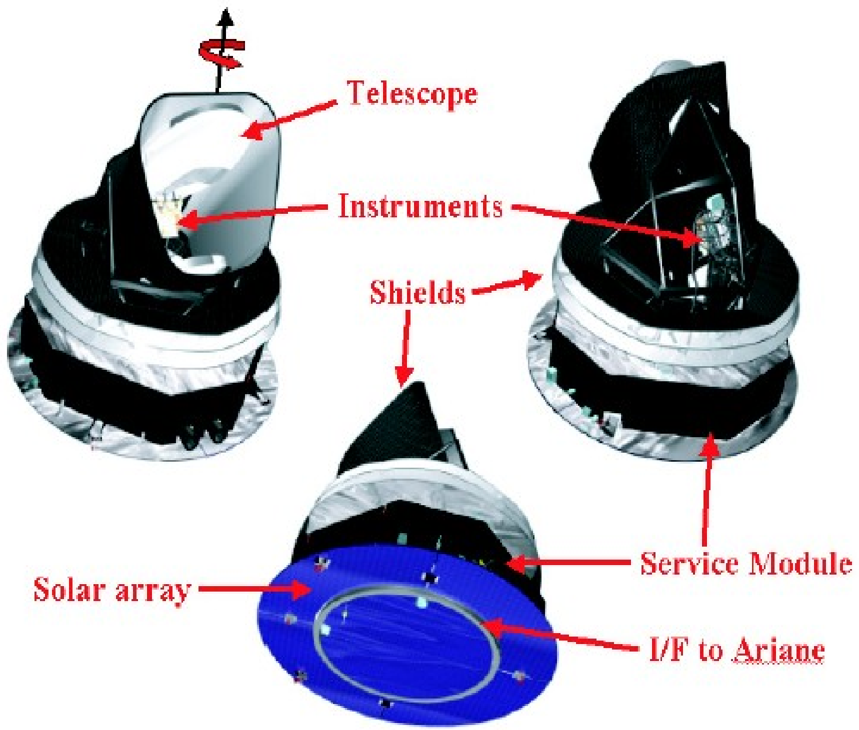

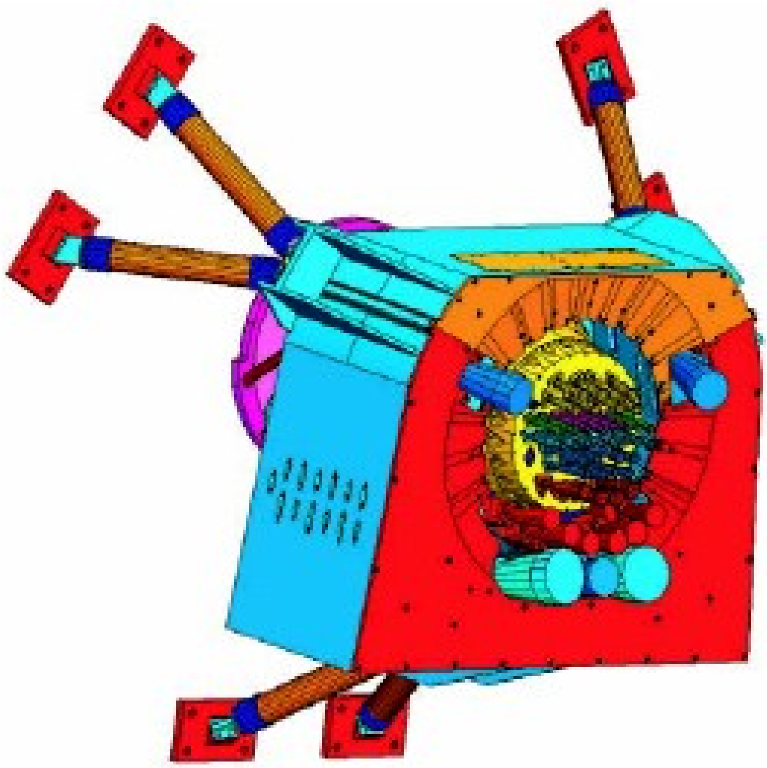

FIG 1.1.— Main elements of *Planck*. The instrument focal plane unit (barely visible) contains both LFI and HFI detectors. The function of the large baffle surrounding the telescope is to control the far sidelobe level of the radiation pattern as seen from the detectors. The specular conical shields (often called "V-grooves") thermally decouple the Service Module (which contains all warm elements of the satellite) from the Payload Module. The satellite spins around the indicated axis, such that the solar array is always exposed to the Sun, and shields the payload from solar radiation. Figures courtesy of Alcatel Space (Cannes).

Planck-LFI: the Instrument

Sensitivity, stability & low systematics

Sensitivity $\Delta T / T \simeq 3 * 10^{-6} / pix$

- State-of-the-art InP LNA technology
- Cryo operation
  20K Sorption Cooler
- 22-element array

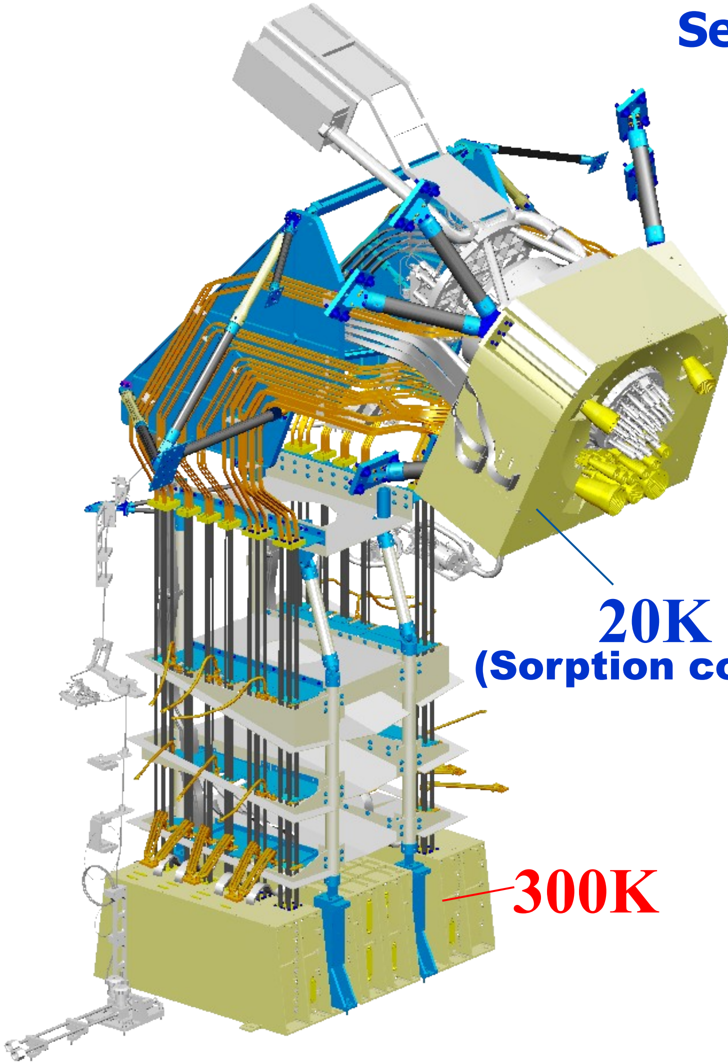

20K
(Sorption cooler)

300K

(MB et al 2010, Mandolesi et al 2010)

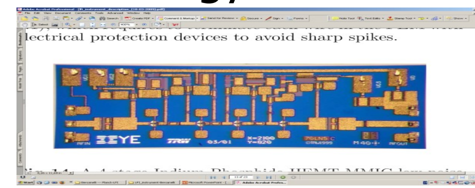

70 GHz MMIC HEMT

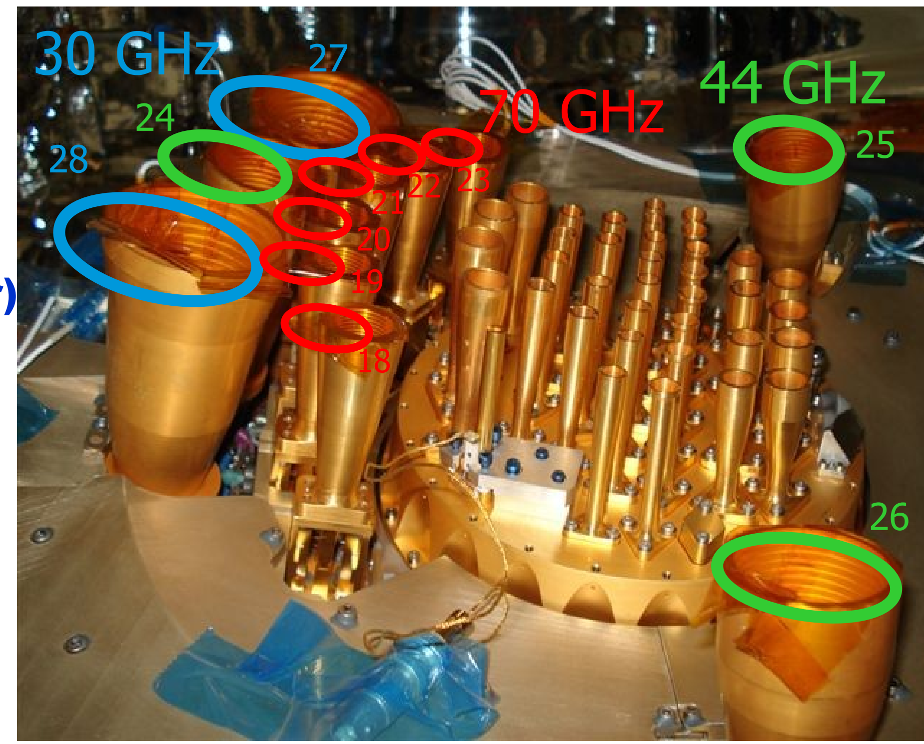

HFI-view

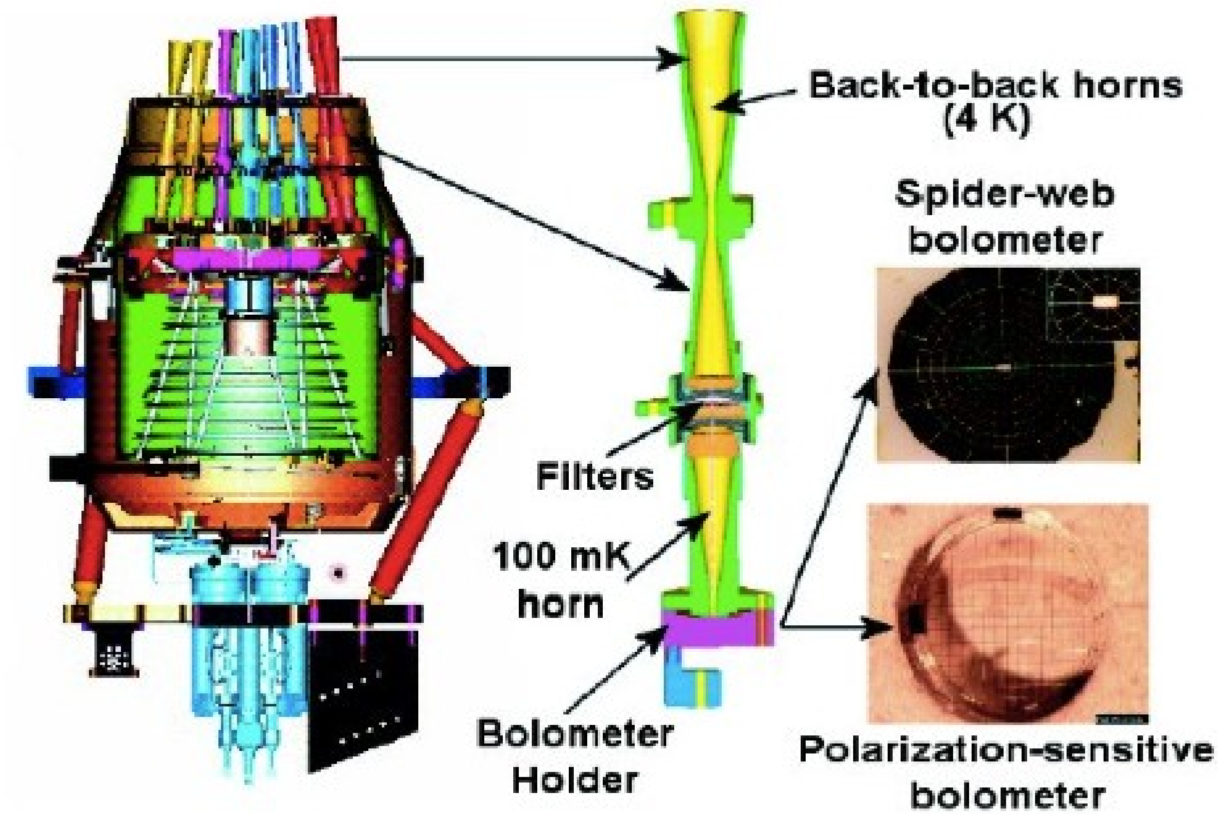

FIG 1.8.—Cutaway view of the HFI focal plane unit. Corrugated back-to-back feedhorns collect the radiation from the telescope and deliver it to the bolometer cavity through filters which determine the bandpass. The bolometers are of two kinds: (a) "spider-web" bolometers, which absorb radiation via a spider-web-like antenna; and (b) "polarisation-sensitive" bolometers, which absorb radiation in a pair of linear grids at right angles to each other. Each grid absorbs one linear polarization only. The absorbed radiant energy raises the temperature of a thermometer located either in the center of the spider-web, or at the edge of each linear grid.

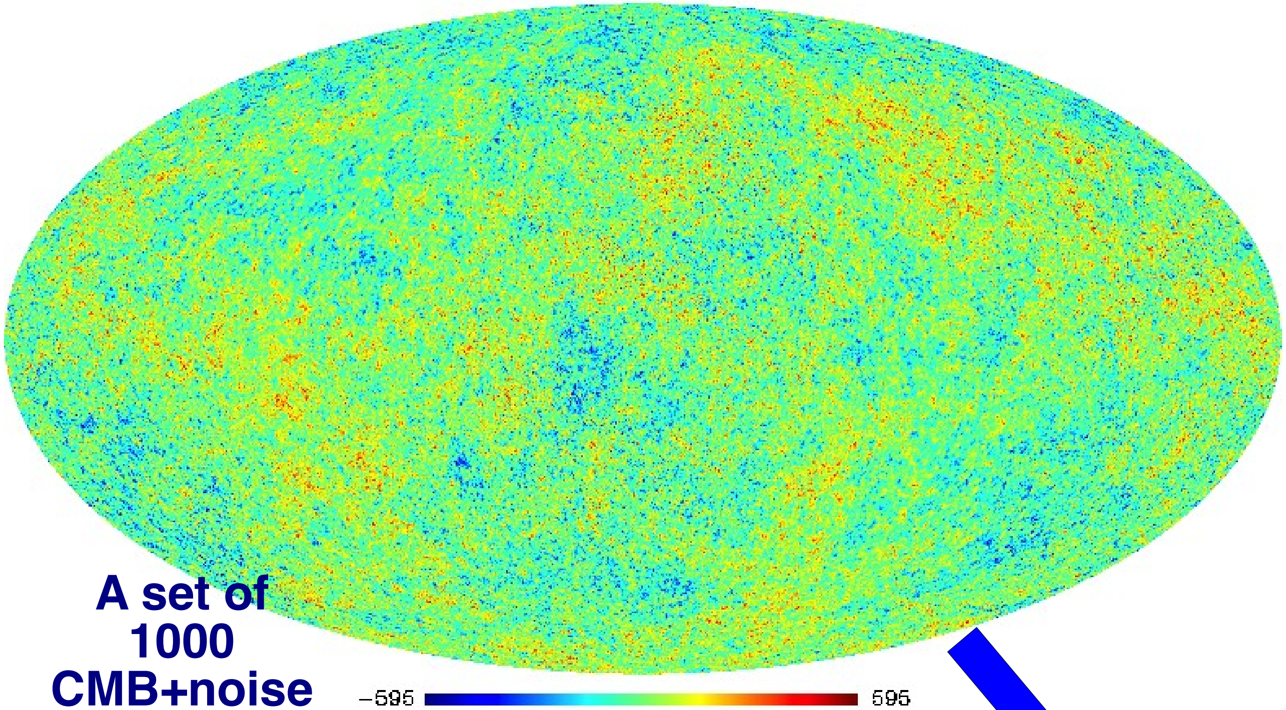

We use the temperature ILC map smoothed and reconstructed at HealPix (Gorski et al. 2005) resolution
N_side = 16, the foreground cleaned low resolution maps and the noise covariance matrix in (Q,U) publicly
available. To perform the analysis, you have to add a masks in temperature and polarization combined them with the Galactic WMAP 9yr low resolution temperature and polarization mask.

A set of 1000 CMB+noise sky realizations has been generated!!

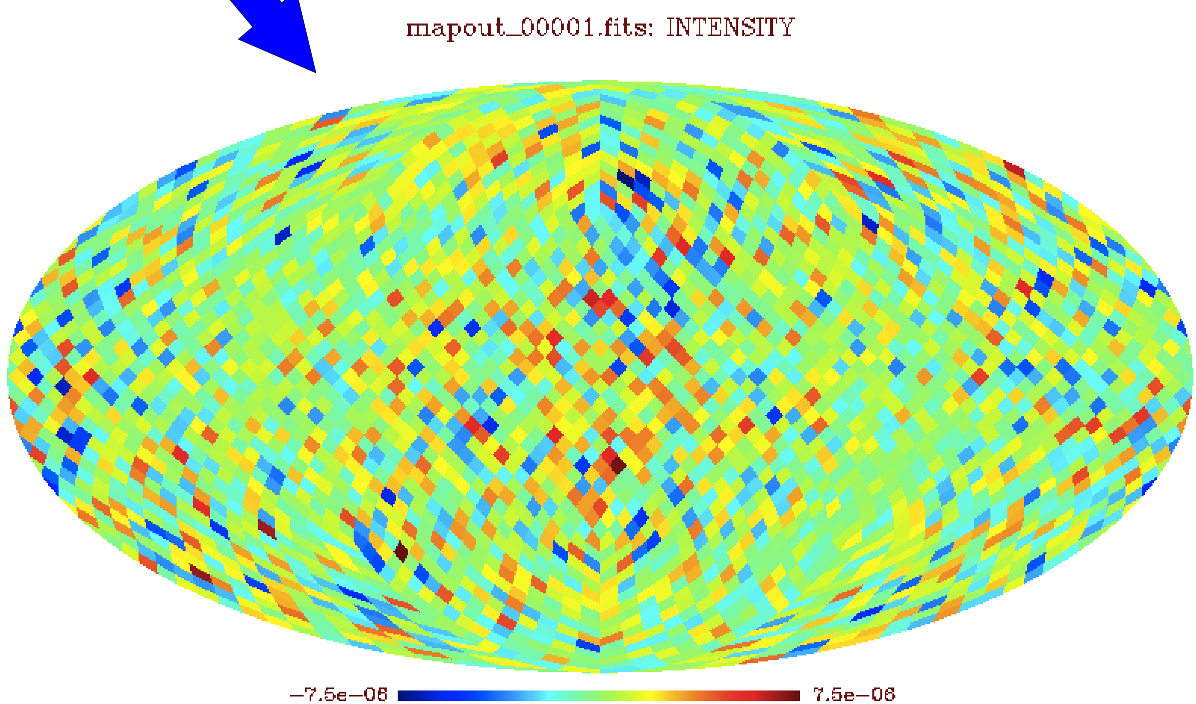

In order to evaluate the angular power spectra, we use the *<u>BolPol</u>* code (Gruppuso et al. 2009), a QML estimator. The QML formalism was introduced in Tegmark (1997) and extended to polarization in Tegmark and de Oliveira-Costa (2001).

Given a map in temperature and polarization x=(T,Q,U), the QML provides estimates the $\hat{C}_l^X$ with X being one of TT, EE, TE, BB, TB, EB - of the angular power spectrum as:

Global covariance matrix (signal+noise)

$$\mathbf{C} = \mathbf{S}(C_l^X) + \mathbf{N}$$

$$\hat{C}_l^X = \sum_{l',X'} (F^{-1})_{ll'}^{XX'} \left[\mathbf{x}^t \mathbf{E}_{X'}^{l'} \mathbf{x} - tr(\mathbf{N}\mathbf{E}_{X'}^{l'}) \right]$$

The Fisher matrix is written as:

$$F_{XX'}^{ll'} = \frac{1}{2} tr \left[\mathbf{C}^{-1} \frac{\partial \mathbf{C}}{\partial C_l^X} \mathbf{C}^{-1} \frac{\partial \mathbf{C}}{\partial C_{l'}^{X'}} \right]$$

$$\mathbf{E}_X^l = \frac{1}{2} \mathbf{C}^{-1} \frac{\partial \mathbf{C}}{\partial C_l^X} \mathbf{C}^{-1}$$

Although an initial assumption for a f ducial power spectrum C_l^X is needed

$$< \hat{C}_l^X > = < \bar{C}_l^X >$$

the average is taken over the ensemble of realizations (or, in a practical test, over Monte Carlo realizations extracted from $\bar{C}_l^X$).

the QML method provides unbiased estimates of the power spectrum contained in the map regardless of the initial guess!!!!!!

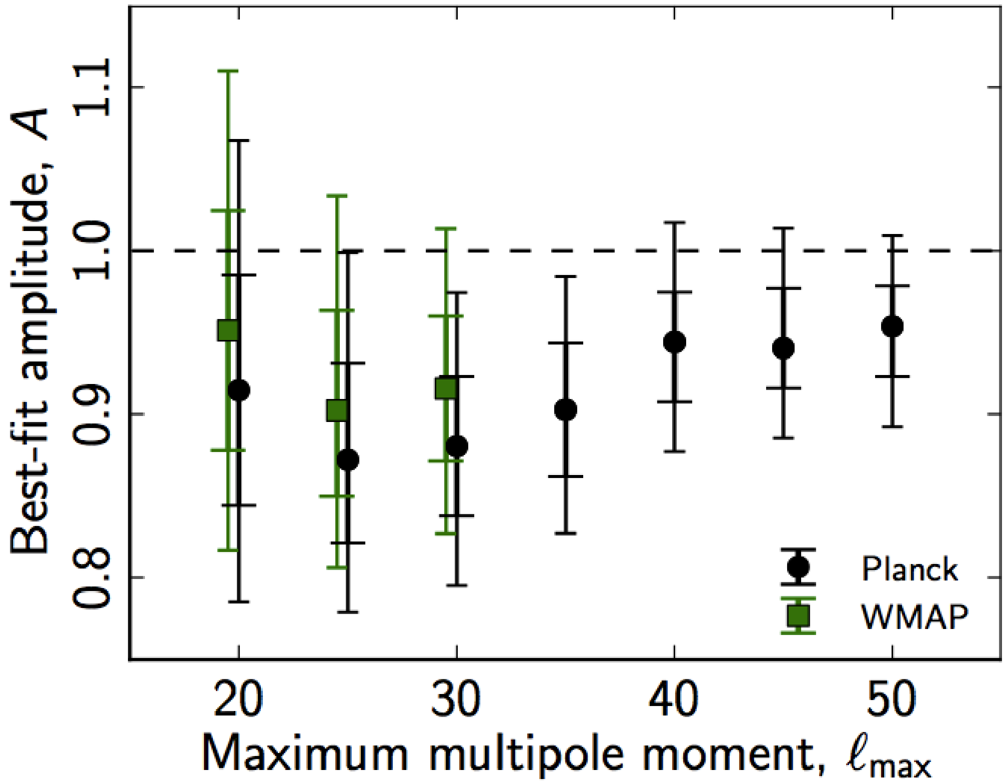

Power spectrum amplitude, relative to the best-ﬁt Planck model as a function of l_max, as measured by the low-l Planck and WMAP temperature likelihoods, respectively. Error bars indicate 68 and 95% conﬁdence regions.

Planck collaboration, arXiv:1303.5075v2 [25 Mar 2013]

We still don't know why there is the a low power respect to WMAP-data: wrong calibration? Some hints for a new physics?
We have to wait for the next year polarization data release (September 2014).

We have a lot of data...how we can use them?

What we can say about physics? Can we learn something about our primordial universe?

- We can constrain cosmological parameters, fundamental constants (the fine structure constant, gravitational constant....)

Physical Processes that Induce CMB Fluctuations

The primary anisotropies of CMB are induced by three principal mechanisms:

- **Gravity (Sachs-Wolfe effect, regions with high density produce big gravitational redshift)**
- **Adiabatic density perturbations (regions with more photons are hotter)**
- **Doppler Effect (peculiar velocity of electrons on last scattering surface)**

The anisotropies in temperature are modulated by the visibility function which is defined as the probability density that a photon is last scattered at redshift z:

$$\frac{\Delta T}{T}(\vec{n}) \doteq \int_0^\infty \left[g(z) \left(\Psi + \Theta_0 + \vec{n} \cdot \vec{\mathrm{v}}_{\mathrm{b}} \right) \right] dz$$

α

Gravity — Adiabatic — Doppler

Visibility function and fine structure constant

$$g(\eta) = \dot{\tau}\ e^{-\tau}$$

Rate of Scattering

$$\dot{\tau}(\eta) = n_e\, x_e\, a\sigma_T$$

Optical depth

$$\tau(\eta) = \int_{\eta}^{\eta_0} d\eta'\, n_e\, x_e\, a\sigma_T$$

$$x_e = \frac{n_e}{n_e + n_H}$$

We can see that the visibility function is peaked at the Epoch of Recombination.

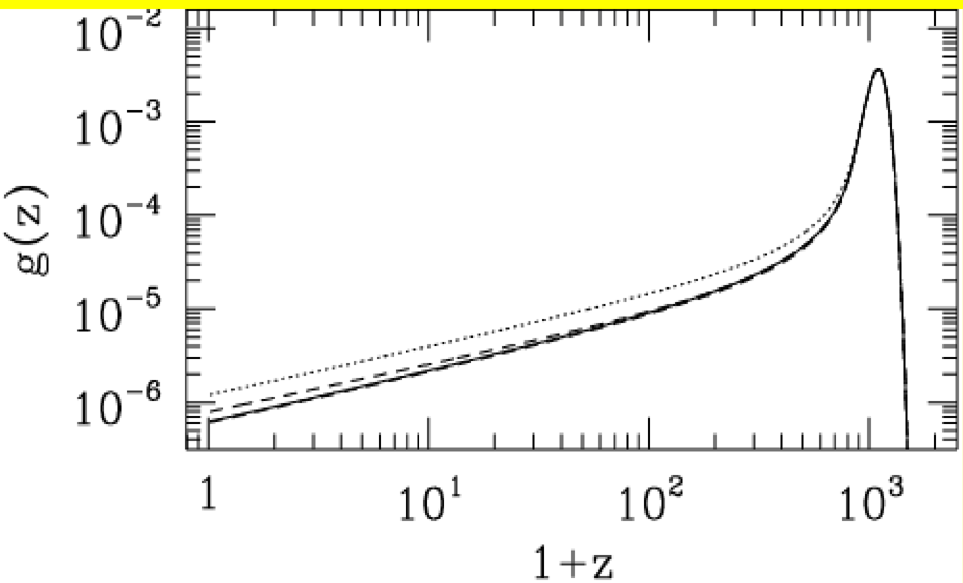

Thomson scattering cross section

$$\sigma_T = \frac{8\pi}{3}\frac{\hbar^2}{m_e^2 c^2}\alpha^2$$

Recombination: standard Model

Direct Recombination

NO net recombination

$$H_{1s} + \gamma \leftrightarrow H^{+} + e^{-}$$

Decay to 2 photons from 2s levels metastable

$$H^{+} + e^{-} \leftrightarrow H_{2s} + \gamma$$

$$H_{2s} \leftrightarrow H_{1s} + 2\gamma$$

Cosmological redshift of **Lyman alpha's photons**

$$H^{+} + e^{-} \leftrightarrow H_{2p} + \gamma$$

$$H_{2p} \leftrightarrow H_{1s} + \gamma$$

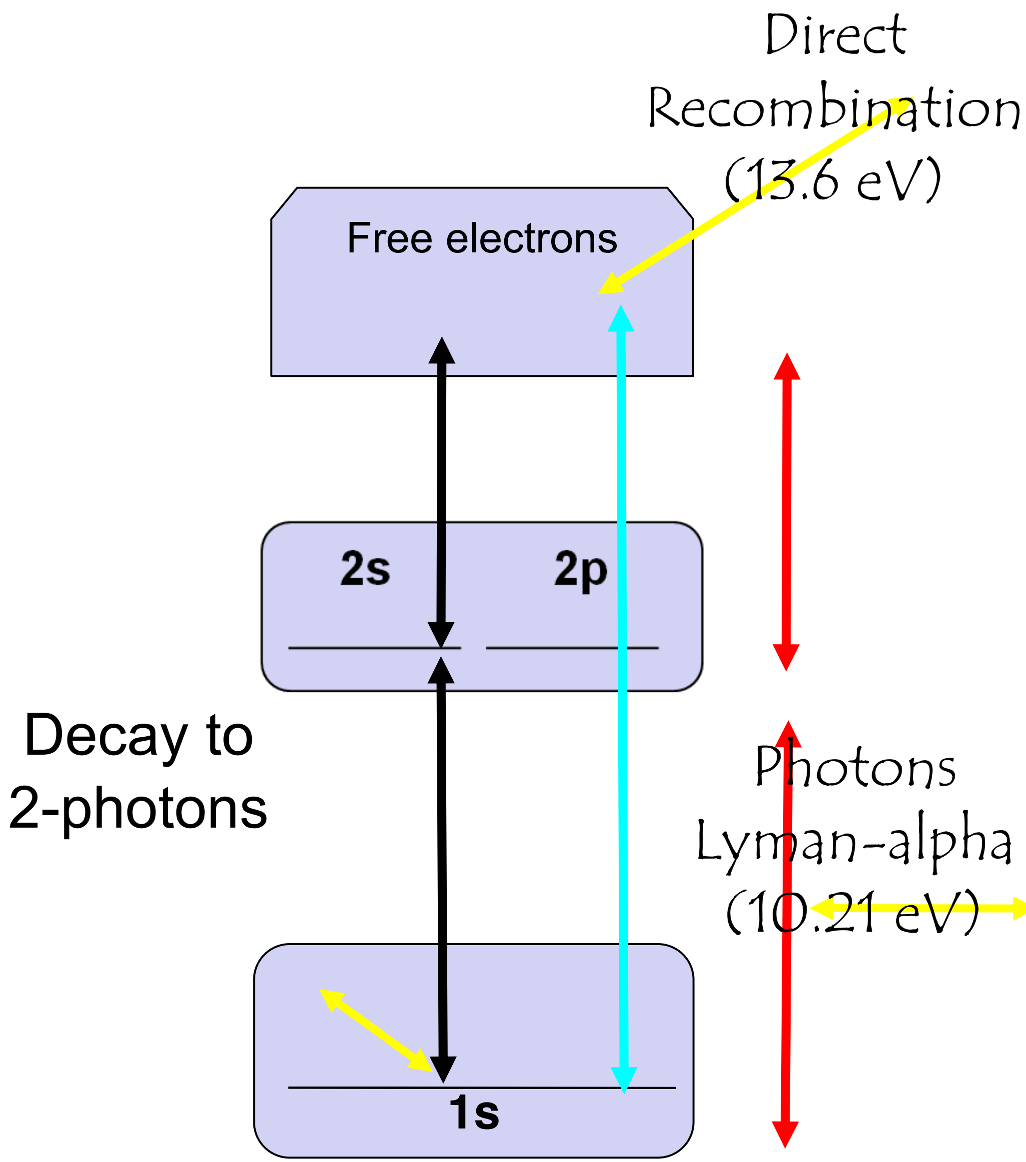

Evolution of the free electron fraction with time

ionization coefficient

$$\beta_H \equiv R_H \left(\frac{2\pi m_e K_B T}{h^2} \right) e^{-B_2 / K_B T}$$

recombination coefficient

$$R_H \approx \sigma_{nl} f(B_n, T)$$

cross section of ionization

$$\sigma_{nl} \propto \alpha^{-1} m_e^{-2} f(h\nu / B_1)$$

$$\frac{dx_e}{dt} = C_H \left[\beta_H (1 - x_e) e^{-\frac{B_1 - B_2}{K_B T}} - R_H n_p x_e^2 \right]$$

$$C_H = \frac{1 + K\Lambda_{2s}(1 - x_e)}{1 + K(\beta_H + \Lambda_{2s})(1 - x_e)}$$

Rate of decay 2s a 1s $\quad \Lambda_{2s} \propto m_e \alpha^8$

Constant K $\quad K = n_e \lambda^3 / (8\pi H) \propto m_e^{-3} \alpha^{-6}$

Lyman-alpha $\quad \lambda_\alpha = 16\pi\hbar / (3 m_e c \alpha^2)$

Variation of free electron fraction

If we plot the free electron fraction versus the redshift, we can notice a different epoch of Recombination for different values of alpha. In particular if the fine structure constant α is smaller than the present value, then the Recombination takes place at smaller z.

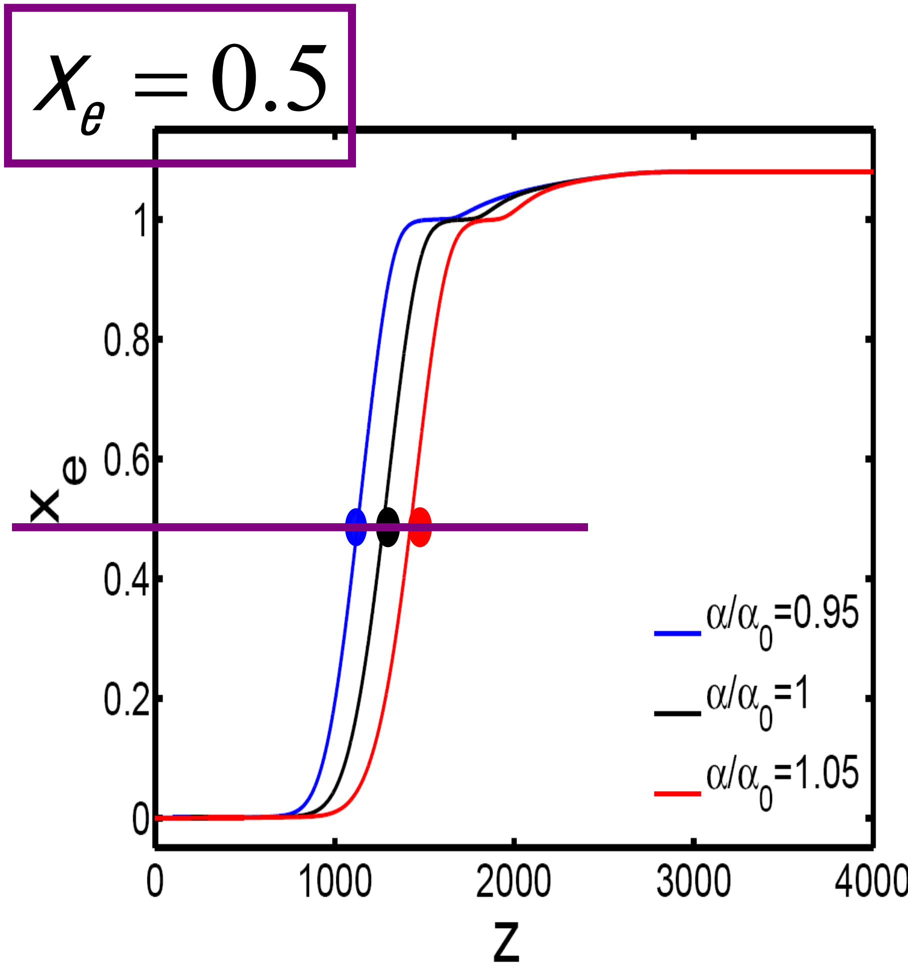

(see e.g. Avelino et al., Phys.Rev.D64:103505,2001)

Modifications caused by variations of the fine structure constant

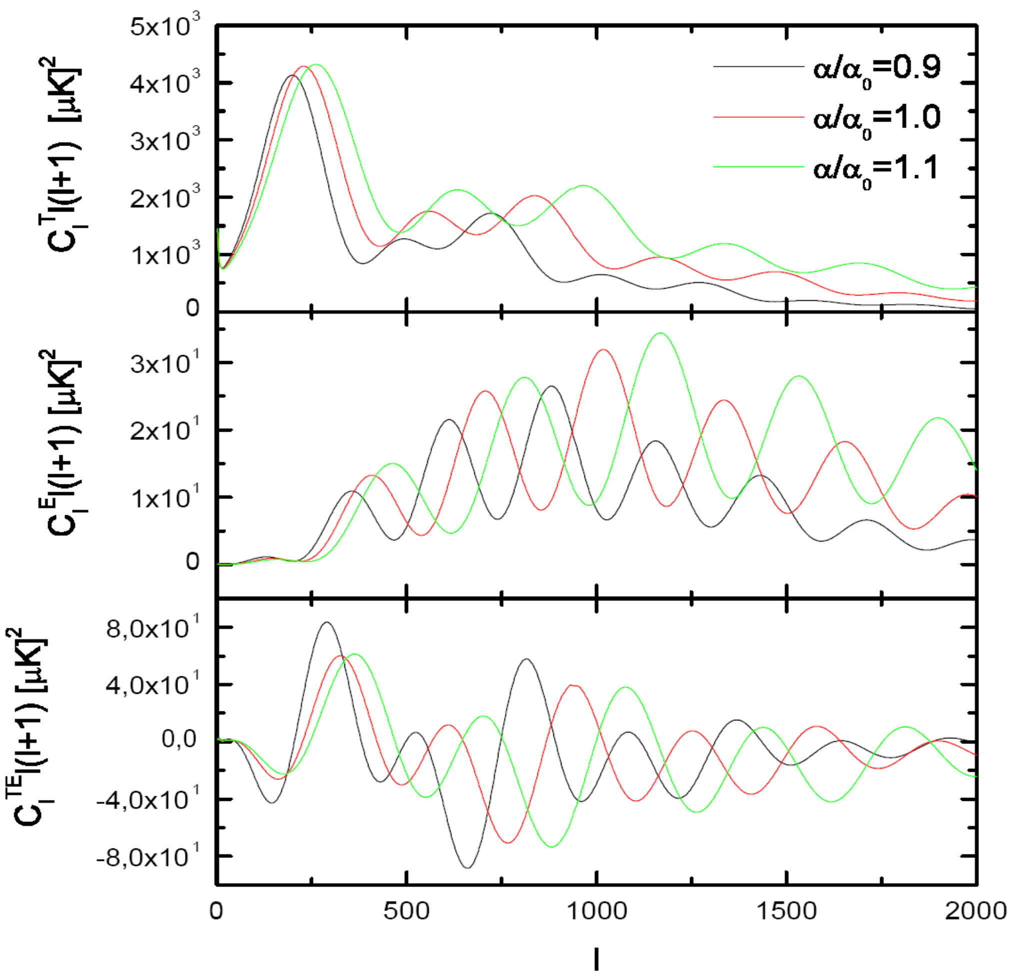

If the fine structure constant is $\alpha/\alpha_0 < 1$ recombination is delayed, the size of the horizon at recombination is larger and as a consequence the peaks of the CMB angular spectrum are shifted at lower l (larger angular scales).

Therefore, we can constrain variations in the fine structure constant at recombination by measuring CMB anisotropies !

Caveat: is not possible to place strong constraints on the fine structure constant by using cmb data alone !

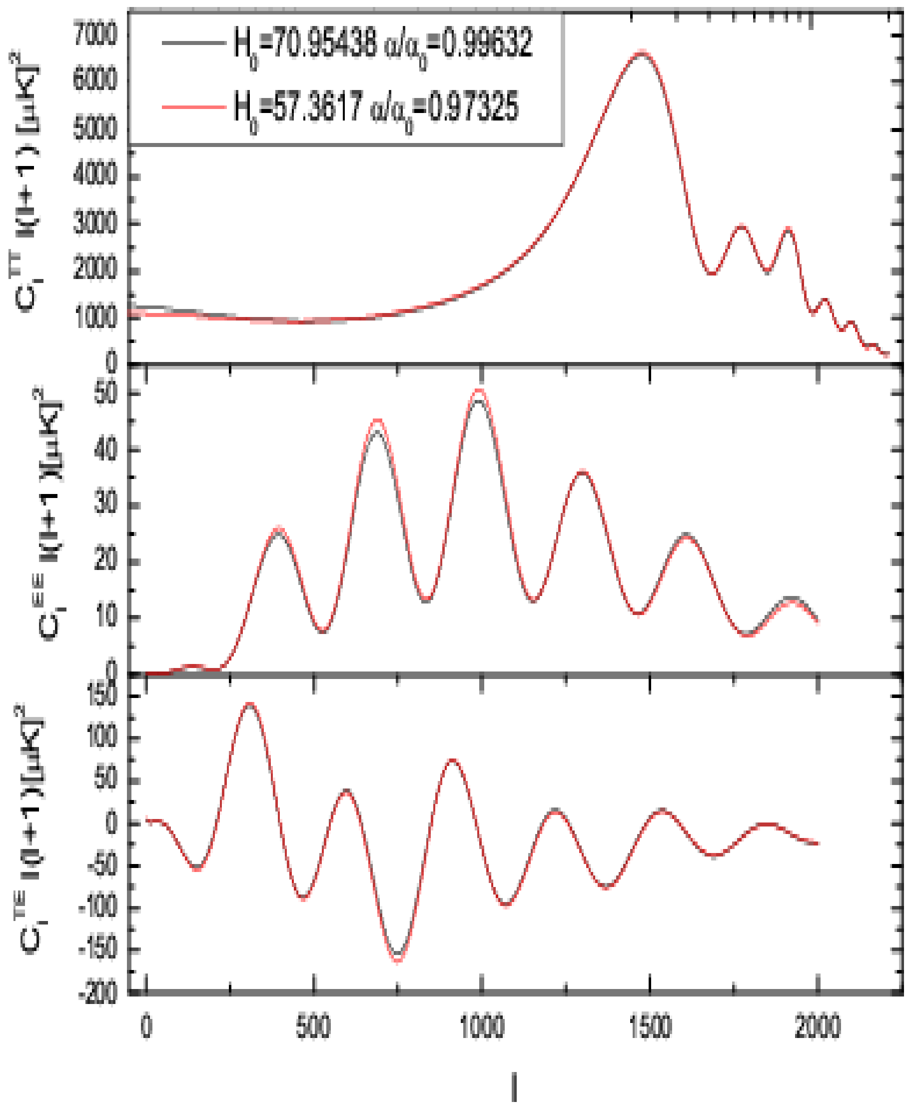

A "cosmic" degeneracy is cleary visible in CMB power spectrum in temperature and polarization between the fine structure constant and the Hubble constant.

The angle that subtends the horizon at recombination is indeed given by:

$$\theta_H \approx c_s H^{-1}(z_r) / d_A(z_r)$$

The horizon size increases by decreasing the fine structure constant but we can compensate this by lowering the Hubble parameter and increasing the angular distance.

New constraints on the variation of the fine structure constant

Menegoni, Galli, Bartlett, Martins, Melchiorri, arXiv:0909.3584v1
Physical Review D *80 081302 (2009)*

We sample the following set of cosmological parameters from WMAP-5 years observations:

Baryonic density	$\Omega_b h^2$
Cold dark matter density	$\Omega_c h^2$
Hubble parameter	H_0
Scalar spectrum index	n_s
Optical depth	τ
Overall normalization of the spectrum	A_s
Variations on the fine structure constant	α / α_0

We also permit variations of the parameter of state w .

We use a method based on Monte Carlo Markov Chain

(the algorithm of Metropolis-Hastings).

The results are given in the form of likelihood probability functions.

We are looking for possible degeneracies between the parameters.

We assume a flat universe.

Constraints on the fine structure constant

In this figure we show the 68% and 95% c.l. constraints on the α / α_0 vs Hubble constant for different datasets .

Experiment	α/α_0	68% c.l.	95% c.l.
WMAP-5	0.998	±0.021	$^{+0.040}_{-0.041}$
All CMB	0.987	±0.012	±0.023
All CMB+ HST	1.001	±0.007	±0.014

TABLE I: Limits on α/α_0 from WMAP data only (first row), from a larger set of CMB experiments (second row), and from CMB plus the HST prior on the Hubble constant, $h = 0.748 \pm 0.036$ (third row). We report errors at 68% and 95% confidence level.

$\approx 0.7\%$

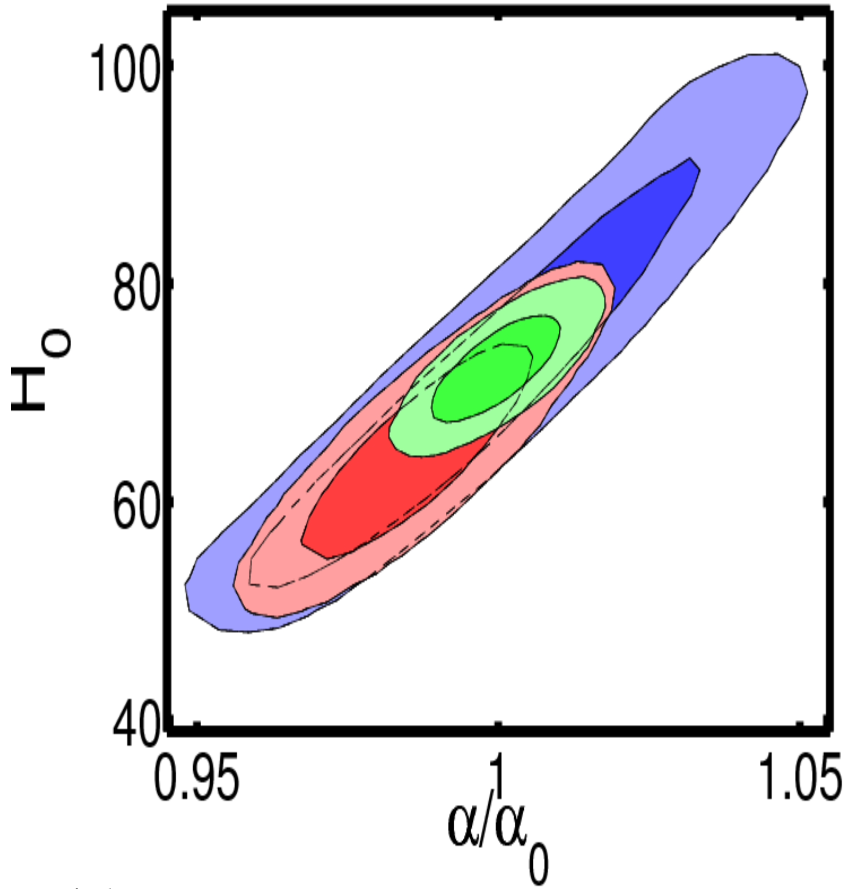

Menegoni, Galli, Bartlett, Martins, Melchiorri, arXiv:0909.3584v1
Physical Review D *80 081302 (2009)*

The degeneracy between the fine structure constant with the dark energy equation of state w

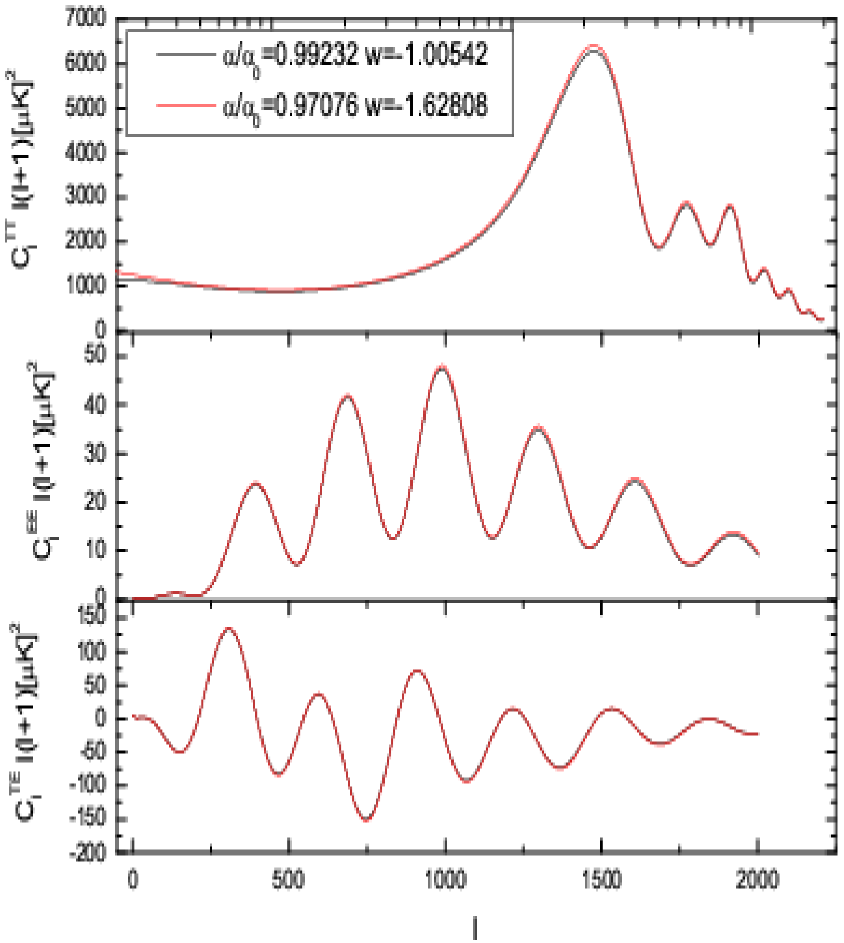

If we vary the value of w we change the angular distance at the Recombination. Again this is degenerate with changing the sound horizon at recombination varying the fine structure constant.

$$d_A = \frac{cH_0^{-1}}{(1+z)} \int_0^{1100} \frac{dz'}{E(z')}$$

$$E(z) = \left[\Omega_m (1+z)^3 + \Omega_r (1+z)^4 + \Omega_X (1+z)^{[3(1+w)]}\right]^{1/2}$$

Constraints on the dark energy parameter w

E. Menegoni, S. Pandolfi, S. Galli, M. Lattanzi, A. Melchiorri
(IJMPD, International Journal of Modern Physics D, Volume 19, Issue 04, pp. 507-512 2010)

Datasets	α/α_0	w
CMB	0.983 ± 0.012	-1.74 ± 0.53
CMB+ HST	0.983 ± 0.011	-1.52 ± 0.39
CMB+ HST+SN-Ia	0.996 ± 0.009	-1.02 ± 0.11

TABLE I: Limits on w and α/α_0 from CMB experiments (first row), from CMB plus the HST prior on the Hubble constant, $h = 0.748 \pm 0.036$ (second row), and from CMB+HST plus luminosity distances of supernovae type Ia from the UNION catalog. We report errors at 68% confidence level.

$\approx 0.9\%$

$\approx 1.1\%$

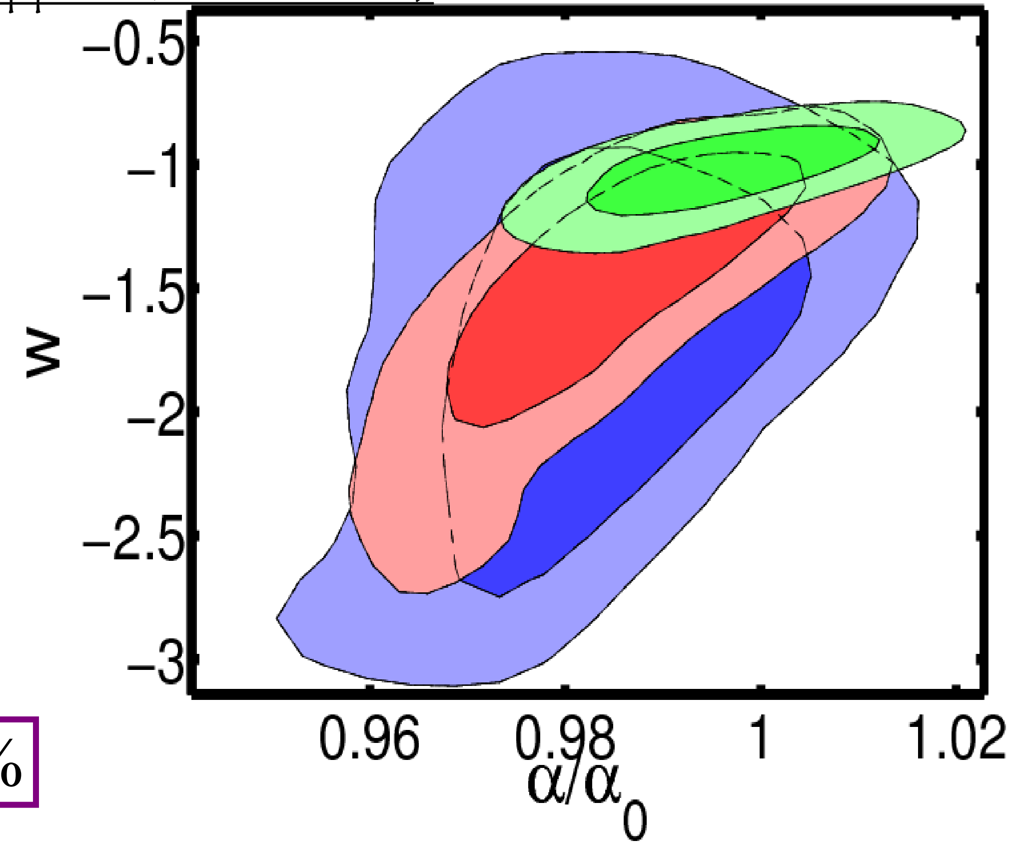

Table 11. Constraints on the cosmological parameters of the base ΛCDM model with the addition of a varying fine-structure constant. We quote ±1 σ errors. Note that for *WMAP* there is a strong degeneracy between H_0 and α, which is why the error on α/α_0 is much larger than for *Planck*.

	Planck+WP	*Planck*+WP+BAO	*WMAP*-9
$\Omega_b h^2$	0.02206 ± 0.00028	0.02220 ± 0.00025	0.02309 ± 0.00130
$\Omega_c h^2$	0.1174 ± 0.0030	0.1161 ± 0.0028	0.1148 ± 0.0048
τ	0.095 ± 0.014	0.097 ± 0.014	0.089 ± 0.014
H_0	65.2 ± 1.8	66.7 ± 1.1	73.9 ± 10.9
n_s	0.975 ± 0.012	0.969 ± 0.012	0.973 ± 0.014
$\log(10^{10} A_s)$	3.106 ± 0.029	3.100 ± 0.029	3.090 ± 0.039
α/α_0	0.9936 ± 0.0043	0.9989 ± 0.0037	1.008 ± 0.020

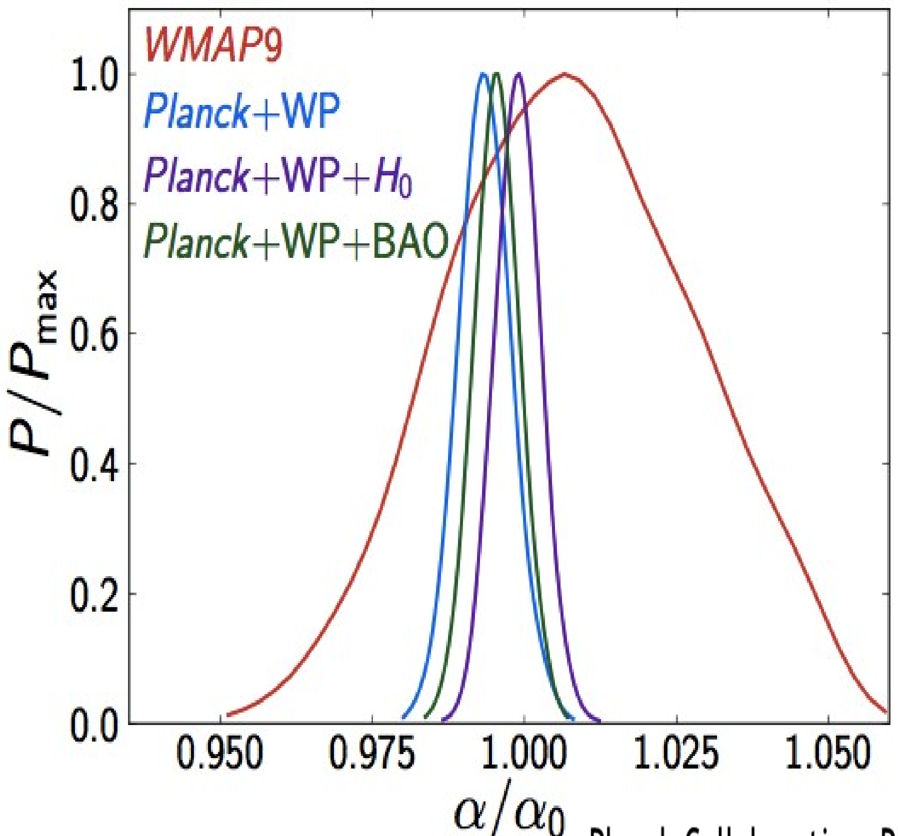

Figure 2. Marginalized posterior distributions of α/α0 for the WMAP-9 (red), Planck+WP (blue), Planck+WP+H0 (purple), and Planck+WP+BAO (green)data combinations.

Planck Collaboration, Planck 2013 results.XVI. Cosmological parameters, arXiv:1303.5076 [astro-ph.CO].

Results from Planck data on α

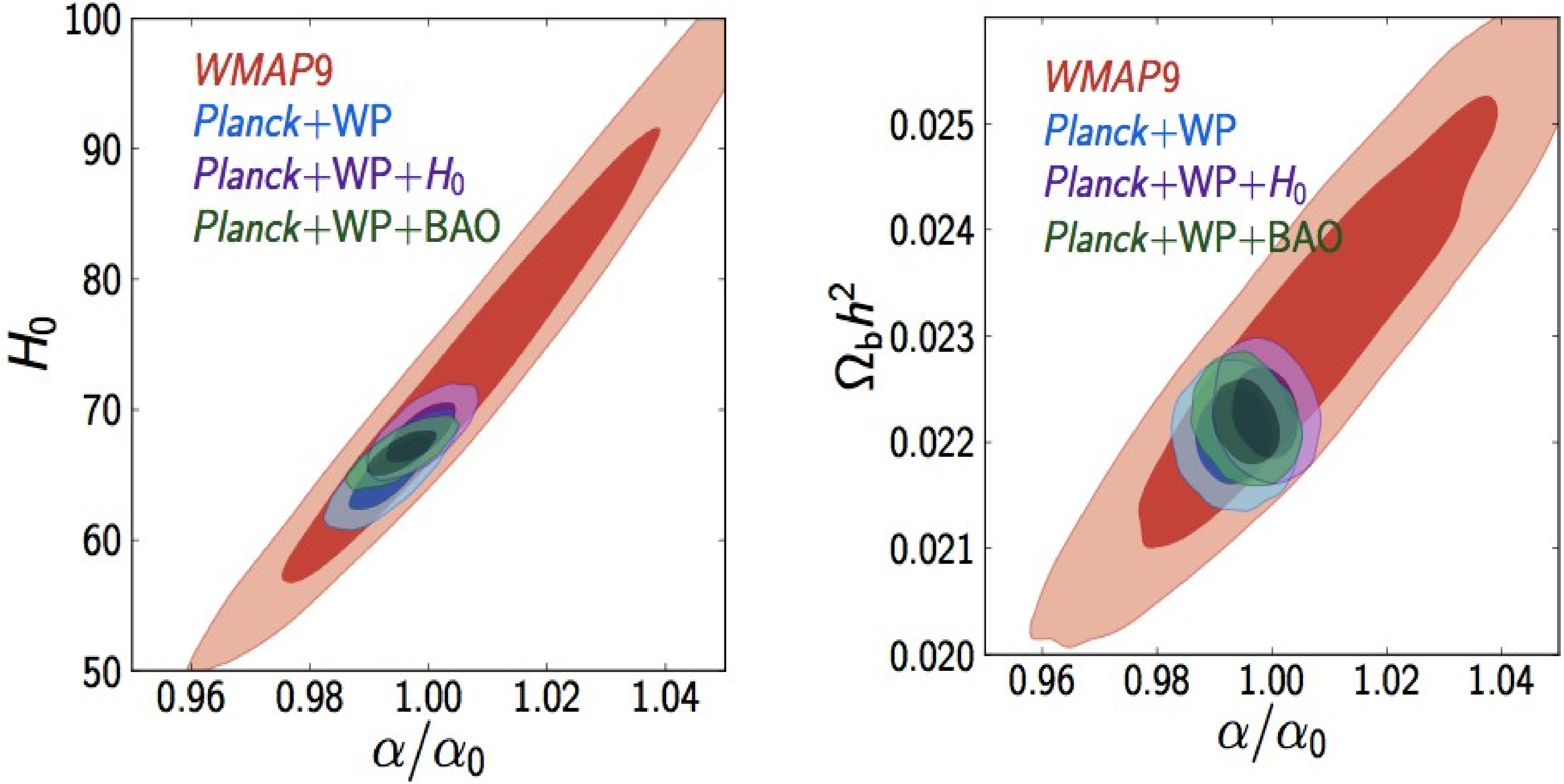

Figure 1. Left: Likelihood contours (68% and 95%) in the α/α_0- H_0 plane for the WMAP-9 (red), Planck+WP (blue), Planck+WP+H0 (purple), and Planck+WP+BAO (green) data combinations Right: As left, but in the α/α_0-$\Omega_b h^2$ plane.

DARK ENERGY MODELS

The standard cosmological model is consistent with the current data only if we admits the presence of a dark energy component

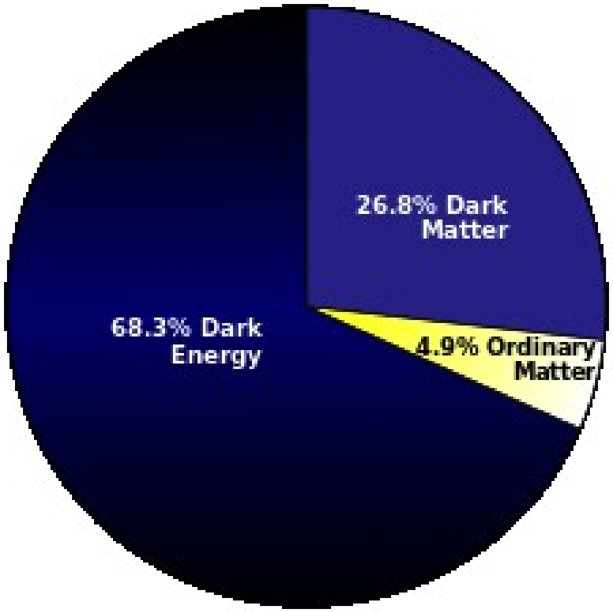

The nature of DE is still a big problem in modern cosmology!!!!

w= -1 OR

w= w(a)

change with time?

- Cosmological constant? Quintessence scalar field?....

Varying fine structure constant: (possible) physical motivations

If dark energy is described by a scalar field, this scalar field can be coupled to the electromagnetic sector and change the value of the fine structure constant

→ In order to have variations of alpha at the Epoch of Recombination we need a scalar field with energy density non-negligible, i.e. **Early dark energy (EDE)**

→ **It's interesting to see what happens to alpha in the case of and EDE component**

DARK ENERGY MODELS

LCDM $w = const = -1$

Scalar field $w = w(a) \neq -1$

The dark energy contribution is assumed to be represented by a scalar field whose evolution tracks that of the dominant component of the cosmic fluid at a given time!

$$\Omega_{\rm de}(a) = \frac{\Omega^0_{\rm de} - \Omega_{\rm e}\left(1 - a^{-3w_0}\right)}{\Omega^0_{\rm de} + \Omega^0_m a^{3w_0}} + \Omega_{\rm e}\left(1 - a^{-3w_0}\right)$$

$$w(a) = -\frac{1}{3[1 - \Omega_{\rm de}(a)]}\frac{d\ln\Omega_{\rm de}(a)}{d\ln a} + \frac{a_{eq}}{3(a + a_{eq})}$$

Calabrese, Roland de Putter, Dragan Huterer, Eric V. Linder, Alessandro Melchiorri

Journal-ref: Phys.Rev.D83:023011,2011

Constraints on the fine structure constant with early dark energy model

The scalar field could be coupled to other components. In this case is taken in account the coupling between the electromagnetism and the scalar field:

$$\frac{\Delta\alpha}{\alpha_0} \equiv \frac{\alpha - \alpha_0}{\alpha_0} = \zeta k(\phi - \phi_0)$$

$$\alpha/\alpha_0(a) = 1 - \zeta \int_a^{a_0} \sqrt{3\Omega_{de}(a)(1 + w(a))}\, d\ln a$$

$$w = -1 + \frac{(\kappa\phi')^2}{3\Omega_{de}}$$

Dark Energy model with a EDE constant component in the past

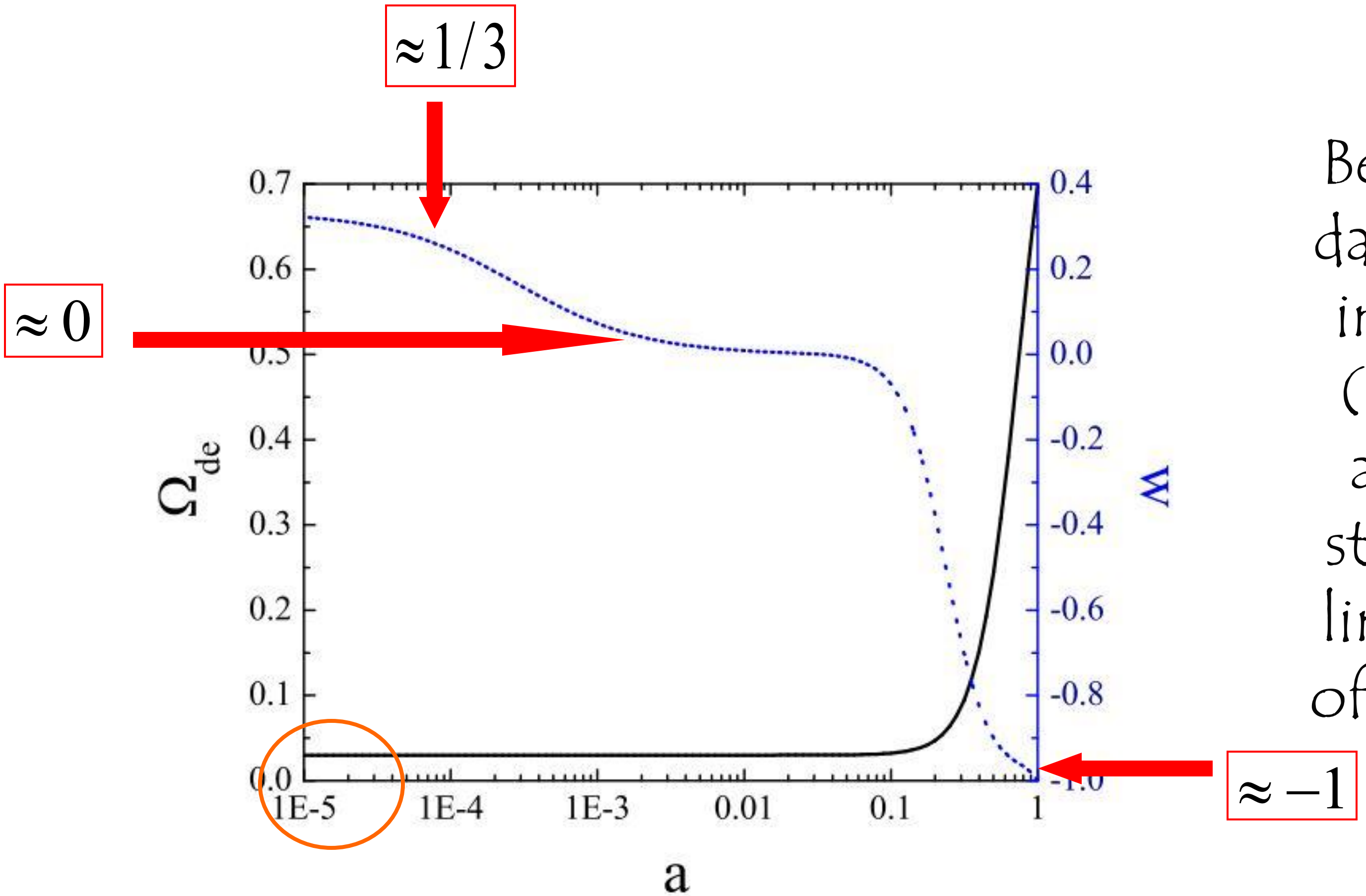

$\Omega_e \approx 0.03$

Behaviour of early dark energy model in energy density (solid black line) and equation of state (dotted blue line) as a function of the scalar factor.

Constraints on the variations of the fine structure constant, EDE density parameter and on coupling

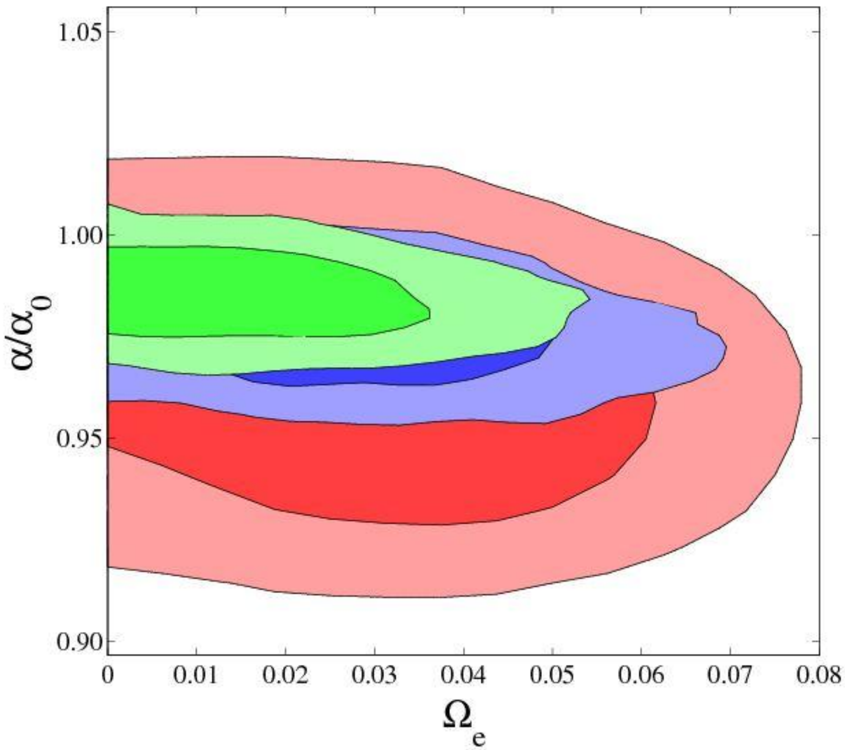

Experiment	α/α_0	Ω_e	ζ
WMAP7+HST	0.963 ± 0.044	< 0.064	< 0.047
WMAP7+ACT+HST	0.977 ± 0.010	< 0.051	< 0.028
WMAP7+ACT+HST+BAO	0.986 ± 0.014	< 0.043	< 0.024

Calabrese, Menegoni, Martins, Melchiorri and Rocha

Phys.Rev.D84:023518,2011

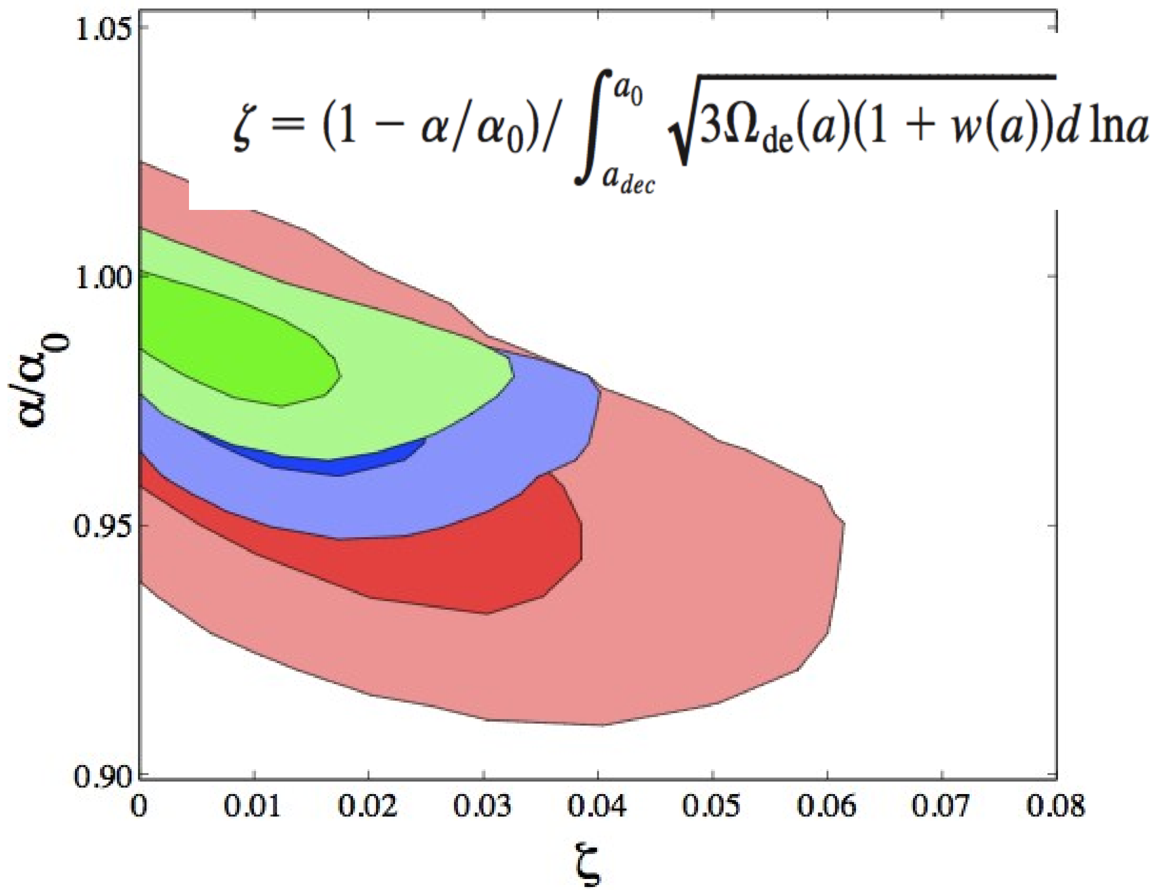

The current constraints are 20 to 40 times weaker than the ones that can be obtained from weak equivalence principle tests..

Our constraints are obtained on completely different scales (cosmological ones as opposed to laboratory ones). So a discrepancy of less than two orders of magnitude is actually impressive!!!! (the Cassini bound effectively on 10^{-4} parsec scales)

TABLE I. Limits at 95% C.L. on α/α_0, Ω_e and the coupling ζ from the MCMC analyses.

Datasets	α/α_0	Ω_e	ζ
WMAP7 + HST	0.963 ± 0.044	<0.064	<0.047
WMAP7 + HST2	0.960 ± 0.040	<0.070	<0.047
WMAP7 + ACT + HST	0.975 ± 0.020	<0.060	<0.031
WMAP7 + ACT + HST + BAO	0.986 ± 0.018	<0.050	<0.025
WMAP7 + ACT + HST2 + BAO	0.986 ± 0.016	<0.050	<0.021

Constraints from next experiments…

- To evaluate future sensitivity to these parameters from CMB it's possible consider noise properties consistent with the Planck and CMBPol experiments. For each channel we consider a detector noise of

$$w^{-1} = (\theta\sigma)^2$$

FWHM (Full-Width at Half Maximum)

Temperature/polarization sensitivity $\Delta T / \Delta P$

Experiment	Channel	FWHM	ΔT	ΔP
Planck	70	14'	12.8	18.3
	100	10'	6.8	10.9
	143	7.1'	6.0	11.4
CMBPol	70	12.0'	0.148	0.209
	100	8.4'	0.151	0.214
	150	5.6'	0.177	0.250
$f_{sky} = 0.85$				

TABLE II: Planck and CMBPol experimental specifications. Channel frequency is given in GHz, FWHM (Full-Width at Half-Maximum) in arc-minutes, and the temperature and polarization sensitivity per pixel in μK.

We use a FISHER matrix approach!!

Resuts for alpha, EDE parameter, and the coupling

We then perform a Fisher matrix analysis [20] to estimate the $1-\sigma$ error for each parameter. We assume a ΛCDM fiducial model : $\Omega_b h^2 = 0.02258$, $\Omega_c h^2 = 0.1109$, $\tau = 0.088$, $H_0 = 71\,\mathrm{km/s/Mpc}$, $n_s = 0.963$ plus the EDE parameters that we fix to : $w_0 = -0.90$, $\Omega_e = 0.03$, $c_s^2 = 1$, $c_{vis}^2 = 0$ and $\alpha/\alpha_0 = 1$.

Experiment	σ_{α/α_0}	σ_{Ω_e}	σ_ζ
Planck	0.0012	0.0036	< 0.0012
CMBPol	0.00025	0.0015	< 0.00022

TABLE III: Fisher matrix errors at 68% c.l. on α/α_0 and Ω_e and upper bounds at 95% on coupling ζ from Planck and CMBPol.

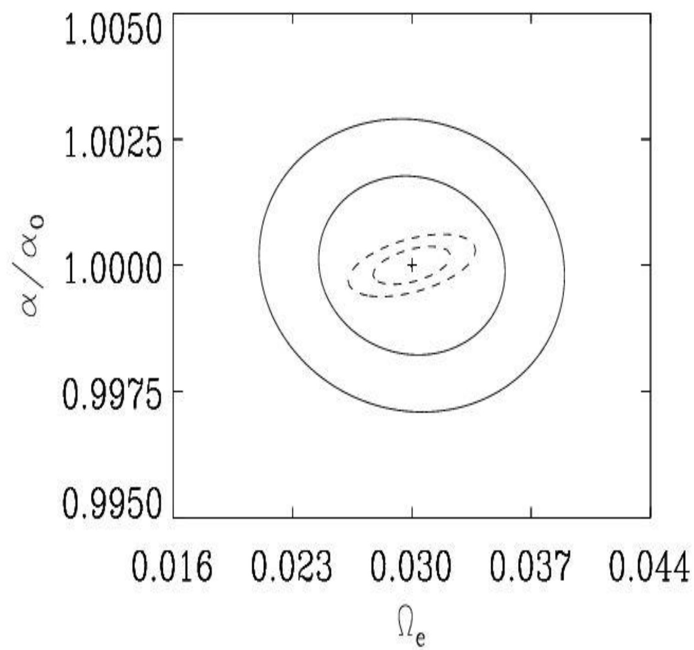

Future constraints on variations of α from combined CMB and weak lensing measurements

Experiment	Channel	FWHM	$\Delta T/T$
Planck	70	14'	4.7
	100	10'	2.5
	143	7.1'	2.2
$f_{sky} = 0.85$			

TABLE I. Planck-like experimental specifications. Channel frequency is given in GHz, the temperature sensitivity per pixel in $\mu K/K$, and FWHM (Full-Width at Half-Maximum) in arc-minutes. The polarization sensitivity is assumed as $\Delta E/E = \Delta B/B = \sqrt{2}\Delta T/T$.

Adding a noise spectrum to each fiducial spectra C_l:

$$N_l = w^{-1} \exp(l(l+1)/l^2{}_b)$$

We combined five quadratic estimators into a minimum variance estimator; the noise on the deflection field power spectrum C_dd ℓ produced by this estimator can be expressed:

$$N_l^{dd} = \frac{1}{\sum_{aa'bb'} (N_l^{aba'b'})^{-1}}$$

Galaxy weak lensing data

Using the Euclid specifications we produce mock datasets of convergence power spectra.
The 1σ uncertainty on the convergence power spectrum (P(ℓ)) can be expressed as:

$$\sigma_l = \sqrt{\frac{2}{(2l+1) f_{sky} \Delta_l}} \cdot \left(P(l) + \frac{\gamma_{rms}^2}{n_{gal}} \right)$$

$n_{gal}(arcmin^{-2})$	redshift	Sky Coverage (square degrees)	γ_{rms}
30	$0.5 < z < 2$	15000	0.22

TABLE II. Specifications for the Euclid like survey considered in this paper. The table shows the number of galaxies per square arcminute (n_{gal}), redshift range, sky coverage and intrinsic ellipticity (γ^2_{rms}) per component.

In our analysis we choose ℓ = 1 for the range2 < ℓ < 100 and ℓ = 40 for 100 < ℓ < 1500. As at high ℓ the non-linear growth of structure is more relevant, the shape of the non-linear matter power spectra is more uncertain therefore, to exclude these scales, we choose ℓmax = 1500. We assume the galaxy distribution of Euclid survey to be of the form $n(z) \propto z^2 \exp(-(z/z_0)^{1.5})$ where z_0 is set by the median redshift of the sources, z_0 = z_m/1.41 with z_m = 0.9.

Model Parameter	Planck Varying α/α_0	Planck $\alpha/\alpha_0 = 1$	Planck+Euclid Varying α/α_0	Planck+Euclid $\alpha/\alpha_0 = 1$
$\Delta(\Omega_b h^2)$	0.00013	0.00013	0.00011	0.00010
$\Delta(\Omega_c h^2)$	0.0012	0.0010	0.00076	0.00061
$\Delta(\tau)$	0.0043	0.0042	0.0041	0.0029
$\Delta(n_s)$	0.0062	0.0031	0.0038	0.0027
$\Delta(\log[10^{10} A_s])$	0.019	0.013	0.0095	0.0092
$\Delta(H_0)$	0.76	0.43	0.34	0.31
$\Delta(\Omega_\Lambda)$	0.0063	0.0050	0.0034	0.0033
$\Delta(\alpha/\alpha_0)$	0.0018	–	0.0008	–

The Euclid future data improves the Planck constraint on α/α_0 by a factor of 2.6!!!

This is a significant improvement since for example, a 2σ detection by Planck for a variation of α could be confirmed by the inclusion of Euclid data at more than 5

standard deviation. The precision achieved by a

Planck+Euclid analysis is at the level of 5×10^{-4}

that could be in principle further increased by the inclusion

of complementary datasets.

M. Martinelli, E. Menegoni, A. Melchiorri, PRD, Vol. 85, No 12, id. 123526 (2012).

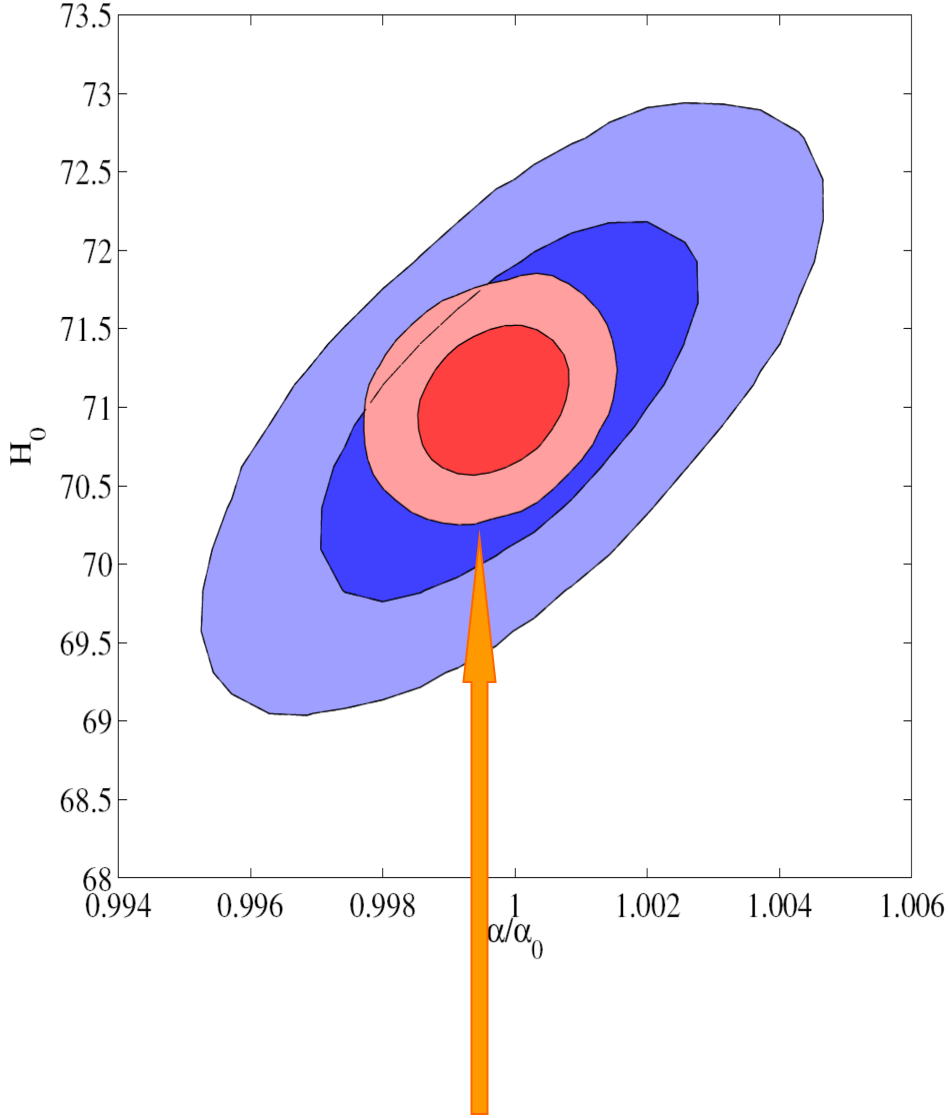

Planck+Euclid

There is a high level of correlation among α/αO and the parameters H_o when only the Planck data is considered. This is also clearly shown in the plot of the 2-D likeihood contours at 68% and 95% c.l. between α/αO and H_o . A larger/lower value for α is more consistent with observations with a larger/lower value for H_o.

Using EUCLID +PLANCK highlights a previously hidden degeneracy between α/αO and τ; both these parameters do not affect the convergence power spectrum, thus they are not measured by Euclid, but they are both correlated with other parameters, such as n_s whose constraints are improved through the analysis of weak lensing. This improvement on ns allows to clarify the degeneracy between α/αO and τ.

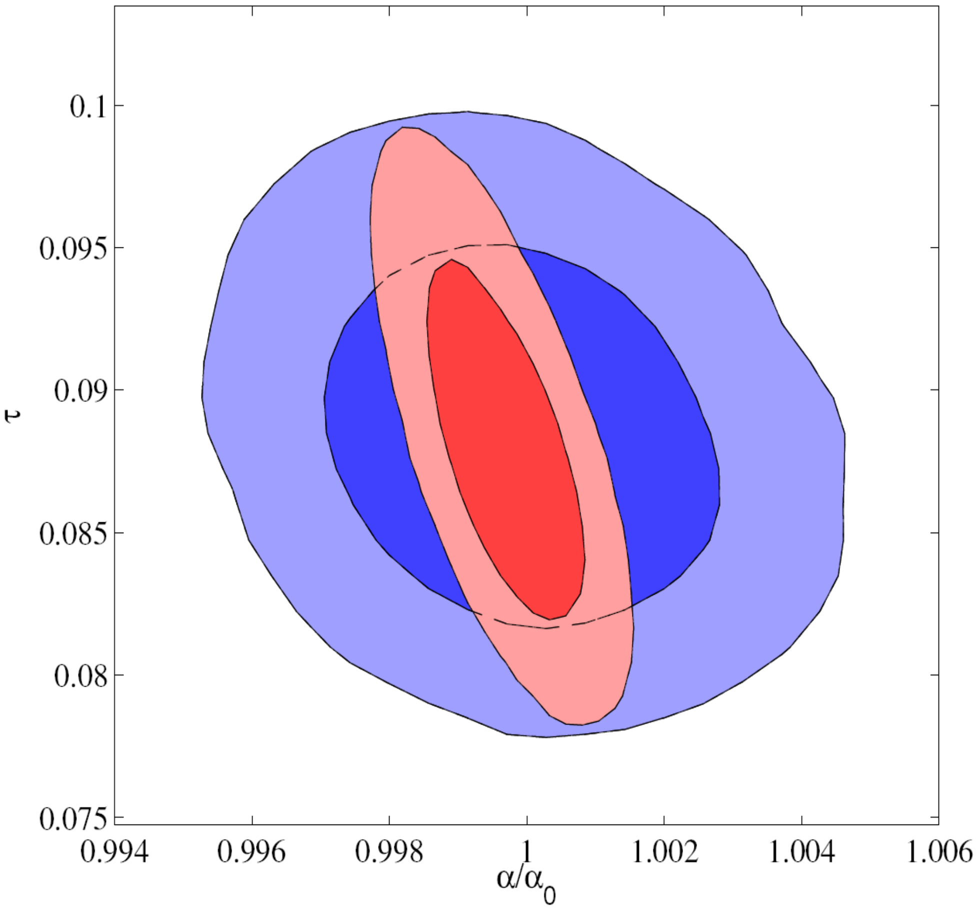

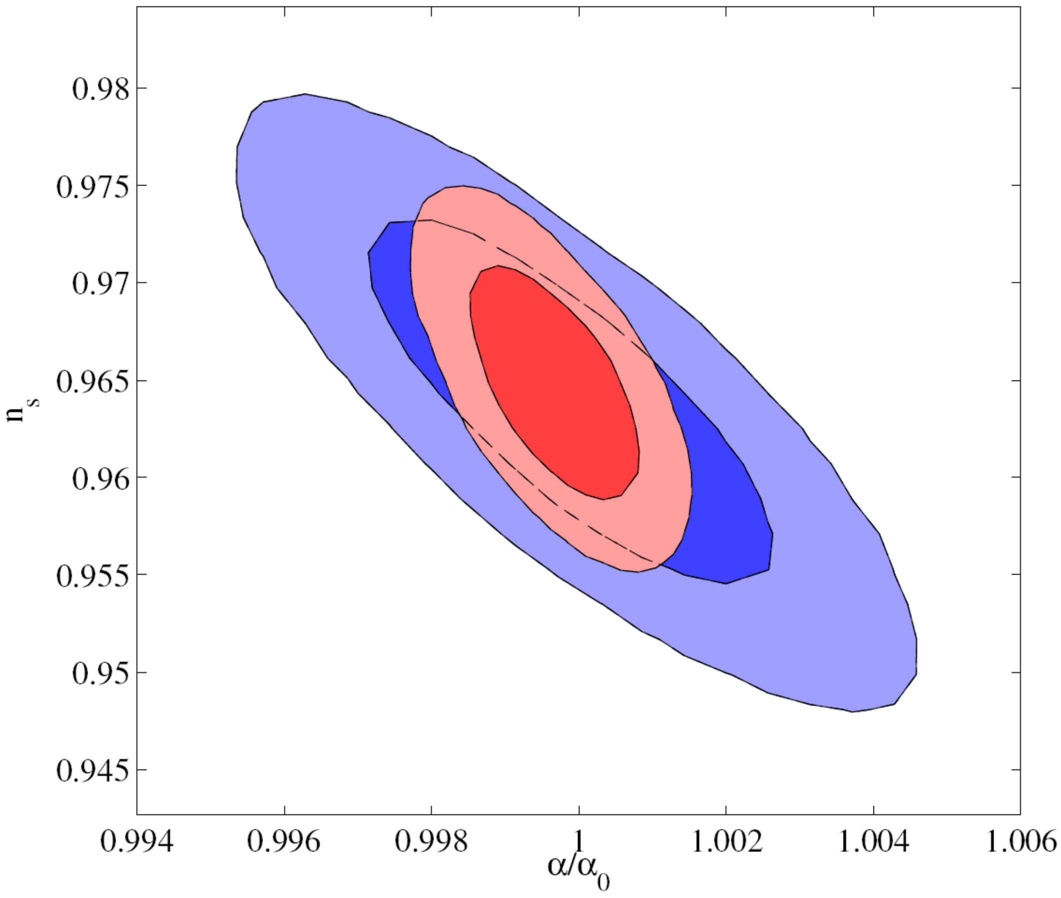

Infact a larger/lower value for α is more consistent with observations with a lower/larger value for n_s!!!!

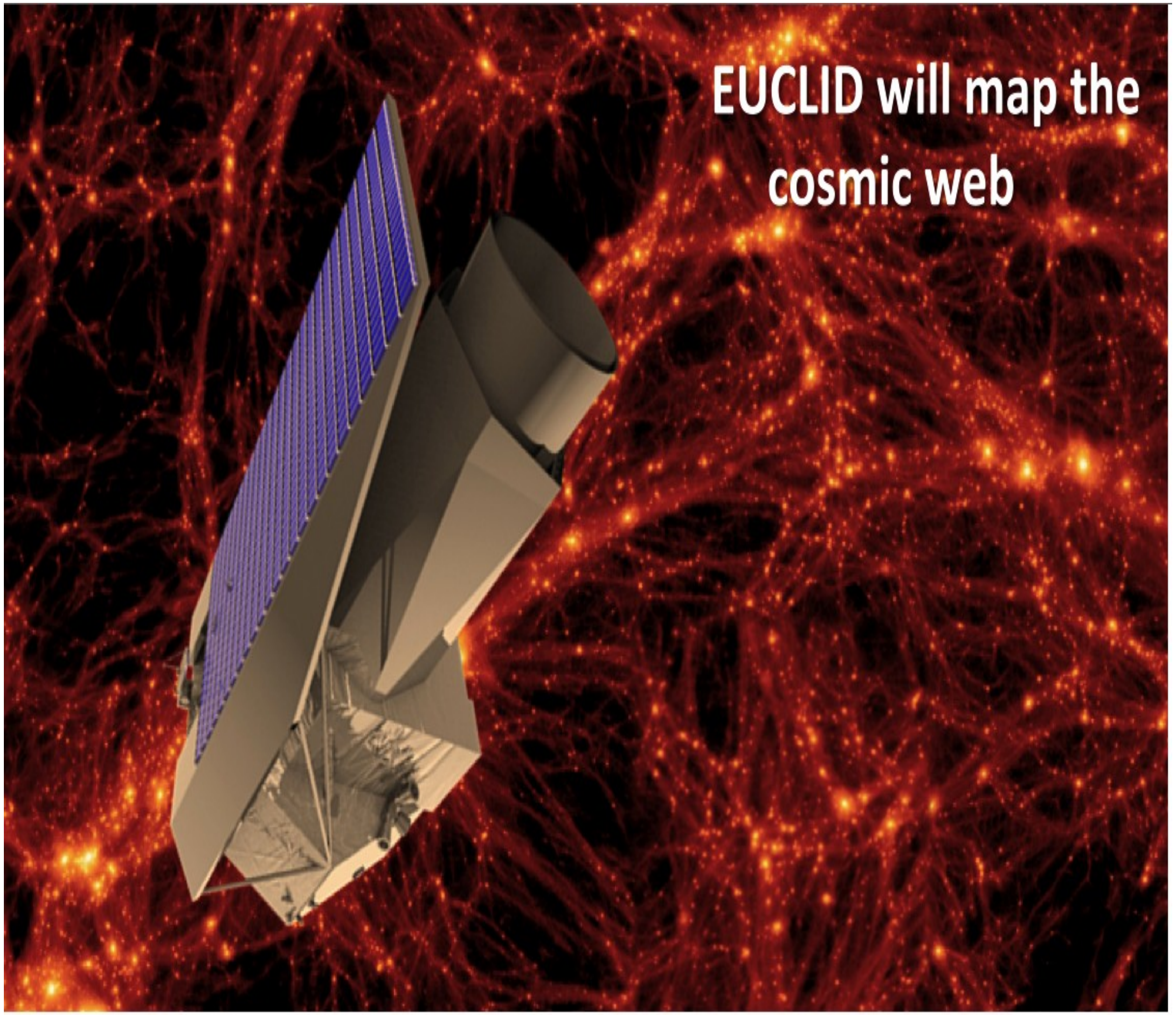

EUCLID will be launched in 2020 to explore **dark energy and dark matter** in order to understand the evolution of the Universe since the Big Bang and, in particular, its present accelerating expansion. Dark matter is invisible to our normal telescopes but acts through gravity to play a vital role in forming galaxies and slowing the expansion of the Universe.

EUCLID+Planck will help in the next future to understand how the structures were originated, and, furthermore to investigate the nature of the dark universe (both matter and energy).

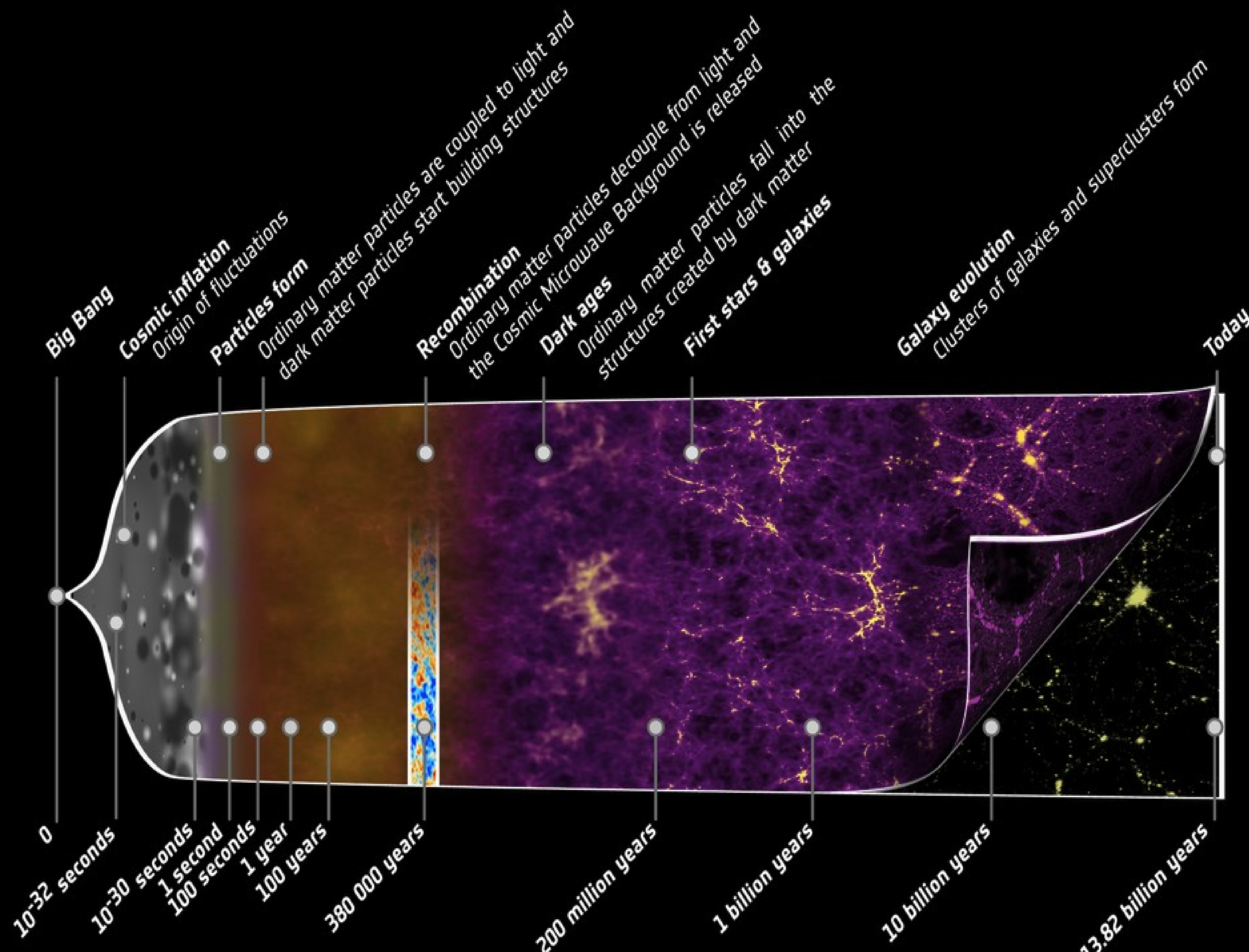

Big Bang
Cosmic inflation
Origin of fluctuations
Particles form
Ordinary matter particles are coupled to light and dark matter particles start building structures
Recombination
Ordinary matter particles decouple from light and the Cosmic Microwave Background is released
Dark ages
Ordinary matter particles fall into the structures created by dark matter
First stars & galaxies
Galaxy evolution
Clusters of galaxies and superclusters form
Today
0
10^{-32} seconds
10^{-30} seconds
1 second
100 seconds
1 year
100 years
380 000 years
200 million years
1 billion years
10 billion years
13.82 billion years

DARK ENERGY MODELS

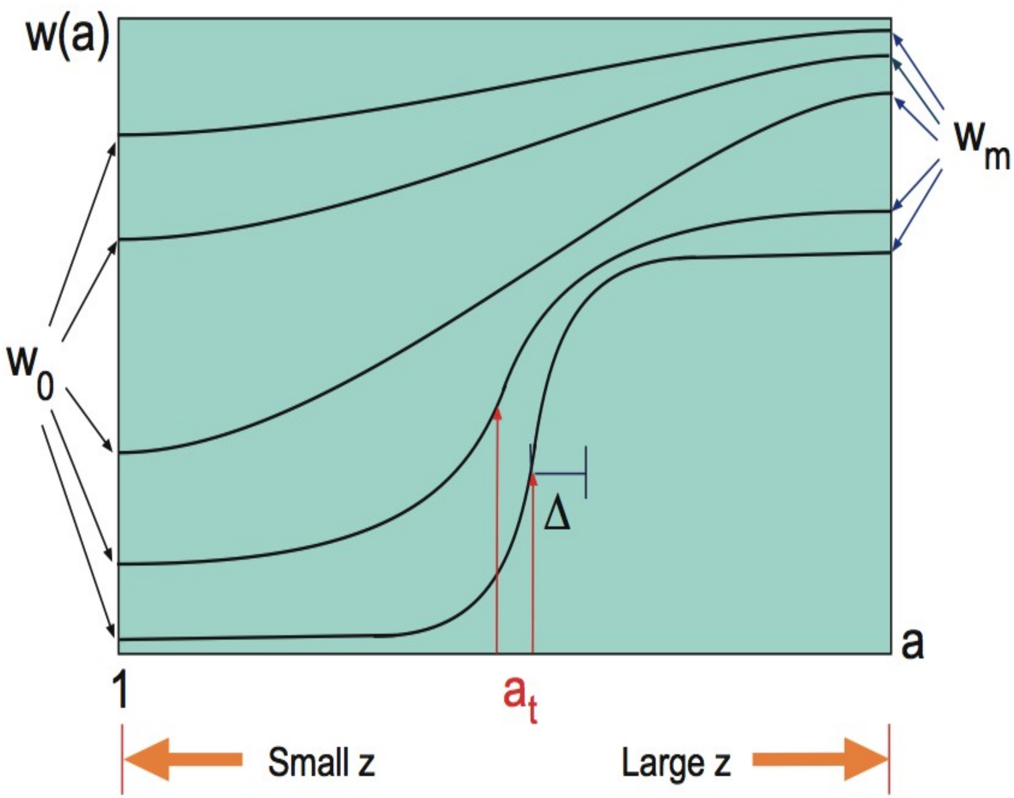

A light scalar field, called **QUINTESSENCE**, rolling down a flat effective potential has been proposed to account for the missing energy in the Universe

QUINTESSENCE MODELS manifesting 'tracker' properties allow the scalar field to dominate the present Universe independently of the initial conditions.

The scalar field evolution:
driven by a non-canonical kinetic term ? and a non-minimal coupling between quintessence and dark matter?
Unified models of dark matter and dark energy?

PS Corasaniti, M. Kunz,D. Parkinson,E.J. Copeland,B.A. Bassett, 10.1103/PhysRevD.70.083006.

CONCLUSIONS:

- We found a substantial agreement with the present value of the fine structure constant (we constrain variations at max of 2,5% at 1-sigma from WMAP-5 years and less than 0.7% when combined with HST observations).

- Planck data improve the constraints on α/α_0 , with respect to those from WMAP-9 by a factor of about five. Our analysis of Planck data limits any variation in the fine structure constant from $z \approx 10^3$ to present day to be less than approximately 0.4%.

- There is no clear degeneracy between the early dark energy density parameter and the fine structure constant, however we can reach tighter constraints on these quantities from the next experiments.

  Combining the data from the Euclid+Planck experiments would provide a constraint of $\alpha/\alpha_0 = 8 \times 10^{-4}$,significatevely improving the constraints expected from Planck. We found that allowing in the analysis for the variations in the fine structure constant has important impact in the determination of parameters as the spectral index, the Hubble constant and the optical depth from a Planck+Euclid analysis.

Thanks for the attention!!!

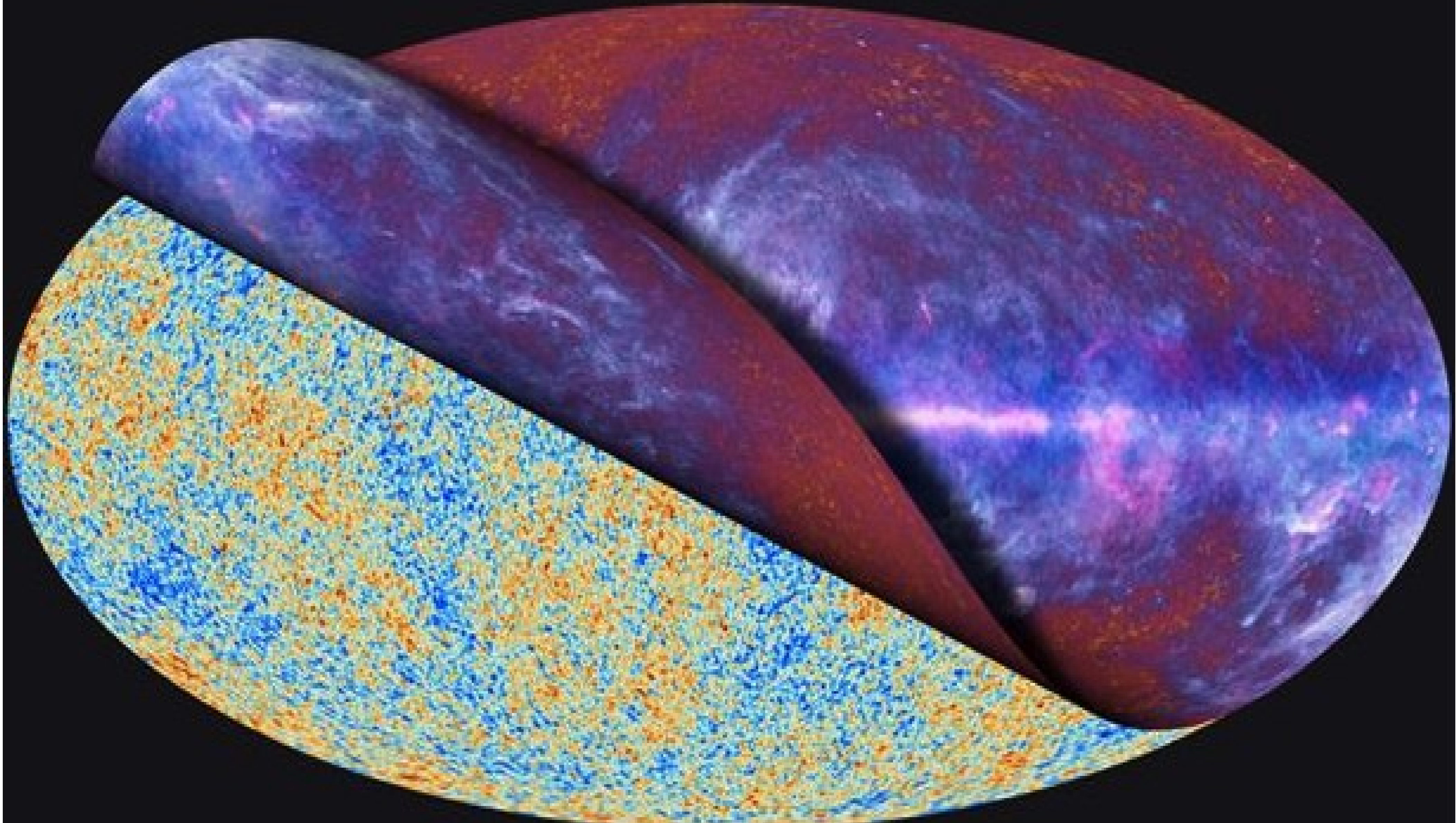

Joyeux Noel!!

The FISHER matrix is defined as

$$L(data|\overline{p})$$

Likelihood function of a set of parameters given some data

$$F_{ij} \equiv \left\langle -\frac{\partial^2 \ln L}{\partial p_i \partial p_j} \right\rangle_{p_0}$$

Parameters of the fiducial model

The Cramèr-Rao inequality implies that $(F^{-1})_{ii}$ is the smallest variance in the parameter p_i .

The one sigma error for each of parameters is defined:

$$\sigma_{p_i} \geq \sqrt{(F^{-1})_{ii}}$$

The FISHER matrix for a CMB experiment is given by

$$F_{ij}^{CMB} = \sum_{XY} \sum_{l=2}^{l_{\max}} \frac{\partial C_l^X}{\partial p_i} (C_l^{XY})^{-1} \frac{\partial C_l^Y}{\partial p_j}$$